2014

Chemkin Simulation of Mercury Oxidation in a Condensing Heat Exchanger

Xingchao Wang
Lehigh University

CHEMKIN SIMULATION OF MERCURY OXIDATION IN A CONDENSING HEAT EXCHANGER

by

Xingchao Wang

A Thesis

Presented to the Graduate and Research Committee

of Lehigh University

in Candidacy for the Degree of

Master of Science

in

Mechanical Engineering and Mechanics

Lehigh University

May, 2014

This thesis is accepted and approved in partial fulfillment of requirements for the Master of Science.

_____

Date Approved

_____

Dr. Edward K. Levy, Thesis Advisor

_____

Dr. D. Gary Harlow, Chairperson of Department

ACKNOWLEDGEMENTS

I would like to highly thank my advisor, Dr. Edward K. Levy, for his continued patience and valuable guidance. Dr. Edward K. Levy let me learn not only the attitude for academic research but also rules of working as an outstanding graduate student. I would also like to thank Dr. Carlos Romero, Mr. Zheng Yao, Mr. Joshua Charles and Mrs. Ursla Levy for their generous help.

Finally, my special thanks to my parents and my family, for their continuous support, understanding and encouragement.

TABLE OF CONTENTS

LIST OF TABLES

LIST OF FIGURES

ABSTRACT

Mercury oxidation in a slip stream condensing heat exchanger (CHX) developed by the Energy Research Center (ERC) at Lehigh University was modeled using hundreds of possible chemical reactions and tens of species in coal-fired power plant furnace and flue gas downstream of the furnace. The modeling tools, CHEMKIN, SENKIN and PSR were used to conduct equilibrium calculations in the furnace and the kinetic calculations in the flue gas leading to the CHX. The detailed mechanism of mercury speciation at the furnace and downstream of the furnace has been investigated. Atomic chlorine is generated in the furnace and flows downstream of furnace, where it reacts with elemental mercury (Hg^0). The predicted results suggest oxidation of Hg^0 in the CHX occurs by this mechanism.

Performance tests of the CHX at Great River Energy's Coal Creek Station were carried out to study moisture, mercury and acid capture abilities of the CHX. The elemental mercury reduction rate and the amount of condensed water were measured in these tests. The measured results show ~35% of Hg^0 was oxidized in the CHX.

The mercury oxidation results show agreement between simulation and test within a typical range of HCl concentration of flue gas at furnace exit from 20 ppmv to 50 ppmv. The kinetic calculations downstream of the furnace show the oxidation reaction between Hg^0 and atomic Cl primarily occurs at temperature 600K to 300K (620°F to 80°F).

The flue gas temperature in the CHX affects condensed water formation and

mercury oxidation rate. An analytical model of heat and mass transfer processes in the CHX was used to obtain predictions of flue gas temperature profiles with different CHX inlet cooling water temperatures.

The simulation results with lower CHX inlet cooling water temperature, which leads to higher flue gas cooling rate and reduced flue gas moisture content in the CHX, suggest higher Hg^0 oxidation rates would be obtained. The predicted Hg^0 reduction rate in the CHX increased to ~42% with CHX inlet cooling water temperature of 35°F and a HCl concentration at the furnace exit of 40 ppmv.

Chapter 1

Introduction

Mercury is one of the most dangerous air toxics due to its toxicity, long-range transport, persistence and bioaccumulation in the environment. Coal-fired power plants are believed to be the largest anthropogenic source of mercury emissions to the air in the U.S., and EPA (United States Environmental Protection Agency)[1] reported over 50% mercury emissions contributed by utility coal boilers from 1990 to 2005, which is shown in Figure 1-1.

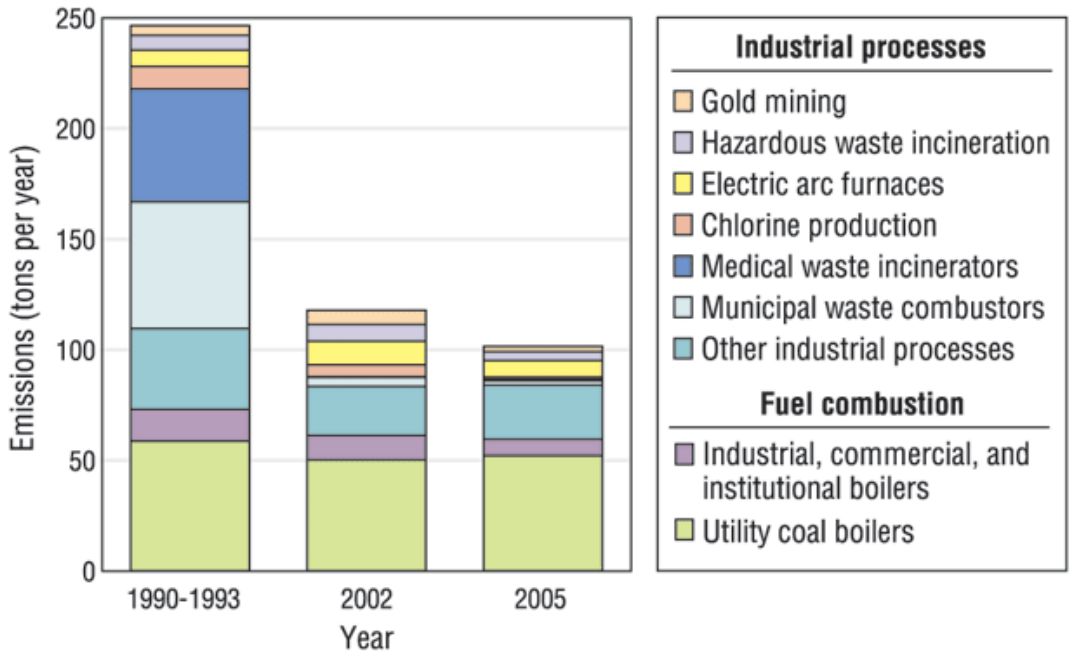

Figure 1-1. Mercury Emissions in the U.S. by Source Category, 1990-1993, 2002 and 2005

Mercury is in trace amounts in coal. In the high temperature regions of boiler, mercury will be released into flue gas from coal as elemental mercury (Hg^0), which is then oxidized by various species in the flue gas. The amount of the total Hg, which is oxidized, has been found from 35 to 90 percent. Oxidized mercury is soluble and likely to combine with the particles in flue gas to form particulate-bound mercury (Hg_p). Therefore, emissions of mercury may be effectively controlled from the downstream of the furnace.

A pilot-scale slipstream condensing heat exchanger (CHX) developed by Energy Research Center at Lehigh University was installed at Great River Energy's Coal Creek Station that has two 550MW lignite-fired units. A test focused on collecting data of Hg speciation and capture within condensing heat exchanger was conducted. The test results and literature indicate Hg^0 was oxidized with ~35% reduction in the flue gas within CHX.

Based on measured mercury oxidation data and an investigation of the mechanism of mercury oxidation of flue gas passing through CHX, equilibrium calculations at the start point (the furnace exit) and Chemkin simulations have been carried out to predict the mercury oxidation rate in the CHX. The mechanism of mercury oxidation downstream of the furnace is briefly discussed in this report. The same initial and inlet conditions for the tests done at Coal Creek station were used in the simulations.

Chapter 2

Literature Review for Mechanism of Gas Phase Mercury Oxidation

The mechanism of mercury oxidation is discussed in this section.

In the high temperature regions of a boiler, Hg will be volatilized and exists as elemental mercury in the flue gas. As the flue gas cools down after combustion, thermochemical equilibrium calculations indicate that Hg^0 is converted to ionic mercury (in the form of $HgCl_2$ or HgO) through gas phase reactions. The parameters impacting on homogenous gas phase Hg^0 oxidation include the flue gas composition, the time-temperature profile, the temperature, and the reaction kinetics.

Hall et al.[1] investigated the potential homogeneous gas phase reactions of mercury and concluded that the main part of Hg^0 will be oxidized by chlorine-containing species like Cl_2 and HCl. Hall et al. also noted that reactions between Hg^0 and NH_3, N_2O, NO, SO_2, H_2S are not a significant factor, however a small amount of oxidation can occur between NO_2 and Hg^0 in coal combustion. According to Galbreath et al.[2] the homogeneous gas phase reaction of Hg^0 and O_2 proceeds at a relatively slow rate of $\leq 1\times10^{-23}$ cm^3 $molecule^{-1}$ s^{-1}.

Since Hg^0 will be primarily oxidized by HCl that is present in coal-fired flue gas and Cl_2 that can be formed in the flue gas, the mechanism of Hg^0 oxidation with HCl and Cl_2 is discussed in detail as below.

For the global reaction between Hg^0 and HCl:

$$Hg + HCl \rightarrow \text{oxidized products}, \quad (1)$$

Lee et al.[3] conducted a bench-scale experiment to study the effects of the flue gas composition on mercury oxidation in simulated flue gas containing HCl. The simulated flue gas used in the tests consisted of 40 ppbv Hg^0, 5% CO_2, 2% O_2, and 93% of N_2 which were all mole fractions. Meanwhile, the effects of SO_2 and H_2O were studied at concentrations of 500 ppmv and 1.7%. HCl concentrations here were 50, 100 and 200 ppmv. This gas phase study indicated that Hg^0 oxidation is very slow in the presence of HCl and occurred only at high temperature (>700℃) and high HCl concentration (>200ppmv). No gas phase oxidation was observed at the temperature below 500℃ with residence time of 3 to 4 seconds. About 27% oxidation of Hg^0 was measured at the highest temperature (754℃) and the highest concentration of HCl (200ppmv). The results also indicated the presence of SO_2 and H_2O inhibit gas phase Hg^0 oxidation.

For the reaction:

$$Hg + Cl_2 \rightarrow HgCl_2, \quad (2)$$

Hall et al.[2] reported that complete gas phase Hg^0 oxidation was observed at temperatures as low as 40℃ with 40 ppmv of Cl_2 at the residence time of 2 seconds. The researchers concluded that Cl_2 is a much more reactive chlorinating agent than HCl. The experiment results also verified the assumption that Cl_2 is an intermediate species in Hg^0 oxidation in the flue gas containing HCl. However, Senior et al.[4] investigated the conversion of HCl to Cl_2 in the flue gas of a coal-fired power plant and concluded that it

is kinetically limited.

Kramlich et al.[5] indicated that the main mechanism for oxidizing Hg^0 to $HgCl_2$ is the reaction of atomic Cl with Hg^0. Kinetic calculations show that atomic Cl is present in high concentration at combustion temperature. As the flue gas cools down, Cl atoms combine to form primarily HCl with minor amounts of Cl_2. Following are elementary reactions occurring in this process.

Intermediate reactions of Cl and HCl:

$$HCl + OH = H_2O + Cl \quad (3)$$

$$HCl + O = OH + Cl \quad (4)$$

$$HCl + M = H + Cl + M \quad (5)$$

$$HCl + O_2 = HO_2 + Cl \quad (6)$$

Intermediate reactions of Cl and Cl_2:

$$Cl_2 + M = Cl + Cl + M \quad (7)$$

$$Cl_2 + O = ClO + Cl \quad (8)$$

$$Cl_2 + H = HCl + Cl \quad (9)$$

The atomic Cl concentration can be calculated by kinetic modeling. Typical results are shown in Figure 2-1 for cooling rates from 100 to 1000 K/s.

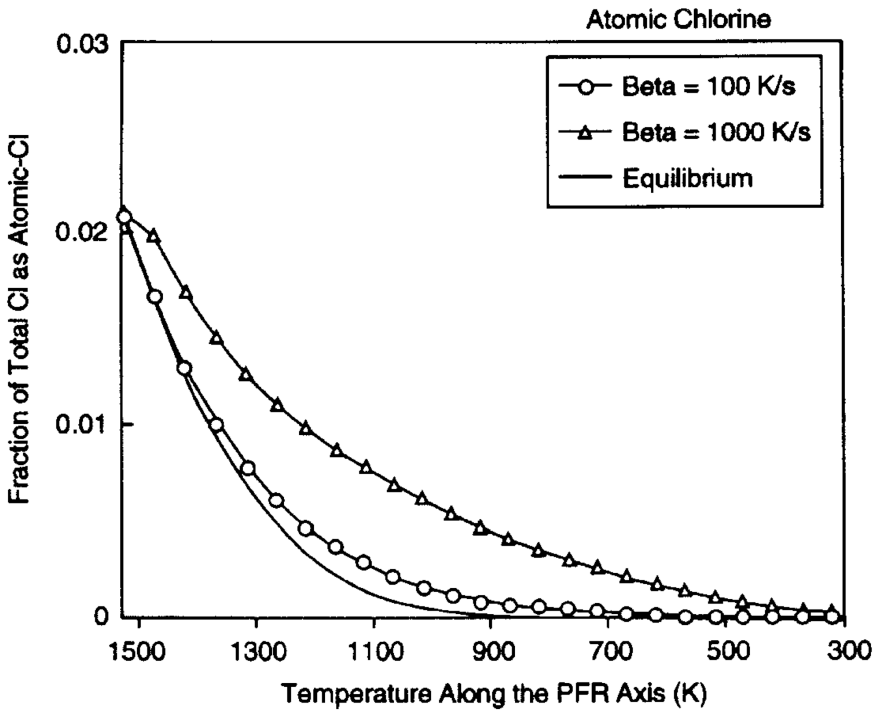

Figure 2-1. Consumption of Atomic Cl during Gas Quenching for Different Values of the Cooling Rate

Kramlich et al.[6] proposed the pathway of homogeneous gas phase mercury oxidation, governed by two steps as below:

$$Hg + Cl\ (+M) \rightarrow HgCl\ (+M) \tag{10}$$

$$HgCl\ + HCl \rightarrow HgCl_2 + H \tag{11}$$

Another reference published by Senior et al.[6] indicated that the reaction of Hg^0 with Cl converts Hg^0 to $HgCl_2$. At furnace temperatures, chlorine in the flue gas exists as gaseous chlorine atoms. It is believed atomic chlorine produced in the furnace flows downstream into lower temperature regions of the boiler and plays a key role in mercury oxidation.

Chapter 3

Mercury Capture Results Measured in Condensing Tests

A slipstream condensing flue gas heat exchanger built by the ERC was installed at Great River Energy's Coal Creek station for two days of testing. Figure 3-1 shows the condensing heat exchanger was made up of six individual heat exchangers and bottles were used to collect condensation from each section.

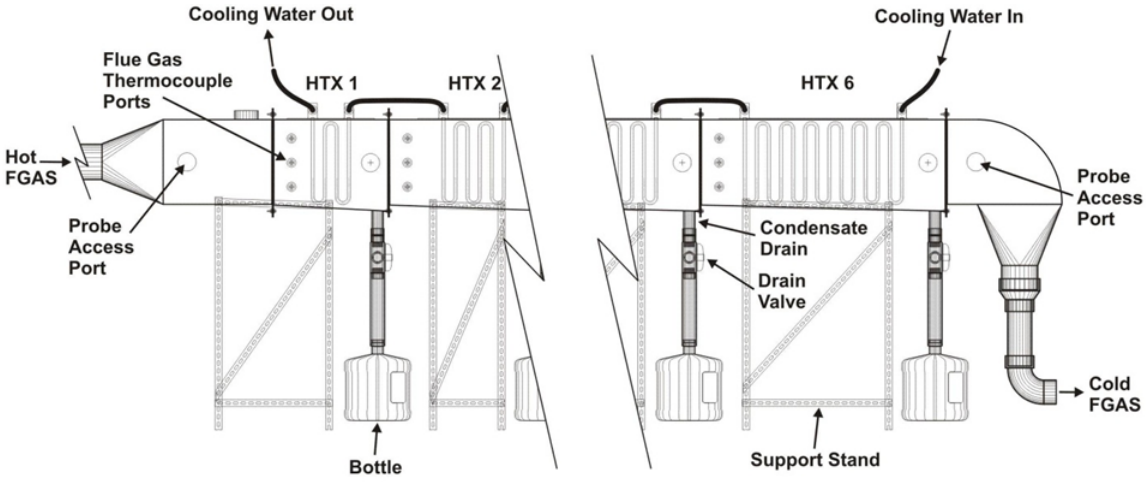

Figure 3-1. Condensing Heat Exchanger System with Six Sections

The geometry of the CHX is presented in Table A-1 in appendix. As shown in Figure 3-2, the flue gas was cooled to approximately 105°F in the low temperature test on 9/27/2012, with a cooling water inlet temperature of nearly 70°F. The cooling water inlet temperature and flue gas outlet temperature on September 28, 2012 were approximately 88°F and 130°F. In these tests, BARR Engineering measured the gaseous SO_x and Hg at the inlet and outlet of the CHX.

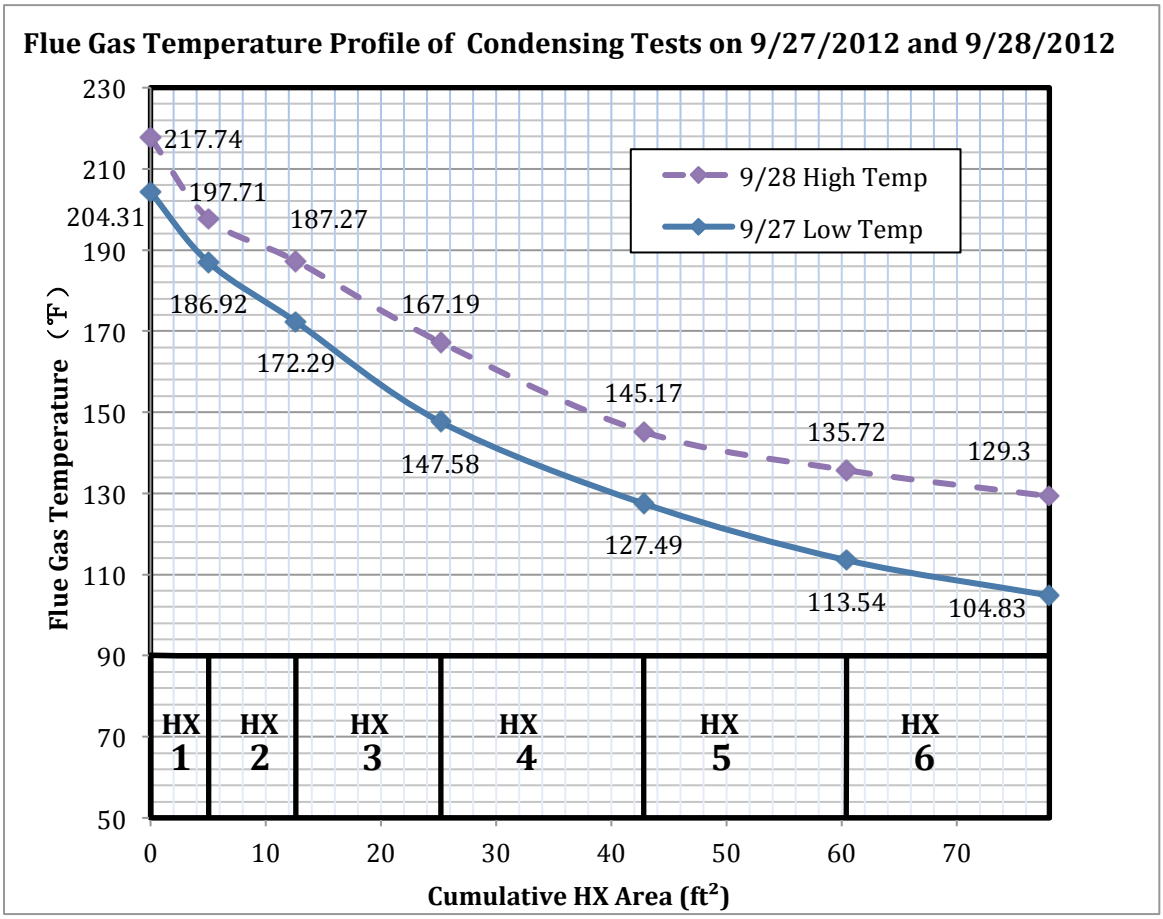

Figure 3-2. Flue Gas Temperature Profile of Condensing Tests on 9/27 and 9/28

Figure 3-2 shows the measured temperature profiles of the condensing heat exchanger in tests done at low temperature on 9/27/2012 and high temperature on 9/28/2012. In each case, it is assumed that the temperature change is linear between inlet and outlet temperatures of each heat exchanger section.

9/27 Low Temperature Test Mercury Changes				
	HTX Inlet	**ΔHg Oxidized**	**ΔHg Captured**	**HTX Outlet**
Elemental Hg [ppbv]	0.797	0.281	-	0.516
Oxidized Hg [ppbv]	0.373	-	0.120	0.255
Total Hg [ppbv]	1.172	-	0.401	0.784
9/28 High Temperature Test Mercury Changes				
	HTX Inlet	**ΔHg Oxidized**	**ΔHg Captured**	**HTX Outlet**
Elemental Hg [ppbv]	0.983	0.320	-	0.663
Oxidized Hg [ppbv]	0.413	-	-	0.518
Total Hg [ppbv]	1.396	-	0.096	1.181

Table 3-1. Mercury Changes Measured in Low Temperature Test on 9/27 and 9/28

Table 3-1 presents measured elemental and oxidized mercury changes as flue gas passed through CHX. It is assumed that any reduction of Hg^0 was due to conversion to $HgCl_2$ during the test. In the test, oxidized Hg was assumed to be captured in the condensed water as flue gas was cooled by cooling water. In the low temperature test, more oxidized Hg was captured than in the high temperature test since more water condensed at low temperature.

The conditions and measured results in the low temperature test have been chosen to study mercury oxidation kinetic modeling.

Chapter 4

Kinetic Modeling of Mercury Oxidation in the CHX

4.1 Introduction to Modeling Tools – Chemkin, SENKIN and PSR

Chemkin is a software tool developed by Sandia National Laboratories for solving complex chemical kinetics problem. It is a highly structured computer package that requires the manipulation of a number of programs, subroutines, and data files, which are shown in Figure 4-1. The Chemkin program essentially integrates the complex gas phase chemical reaction mechanism into numerical simulations. Generally, users are required to input Kinetic Mechanism and Thermodynamic Database. Then, the Chemkin Interpreter reads the user's symbolic description of the reaction mechanism, where the pre-exponential factor A_i, the temperature exponent b_i, and the activation energy E_i are specified which all are the variables of Equation 12.

$$k = A_i T^{b_i} \exp\left[\frac{-E_i}{kT}\right] \quad (12)$$

The parameter values of mercury oxidation mechanism used in the study of this report are attached in Table A-2 in appendix.

SENKIN is a subroutine of Chemkin which predicts the homogeneous gas phase chemical kinetics with sensitivity analysis. In this report, it was used in the economizer, the APH and the CHX to investigate species concentration in the gas phase mercury oxidation with inlet temperatures, residence times and cooling rate.

PSR (Perfectly Stirred Reactor) is also a subroutine of Chemkin predicts the

steady-state temperature and species composition in a perfectly stirred reactor. Input parameters include the reactor volume, residence time, pressure, temperature, and the incoming mixture composition. In this report, a PSR was used to simulate the boiler to obtain the equilibrium flue gas composition at the furnace exit.

Figure 4-1 shows the structure of Chemkin program package and the link to SENKIN. The Application Code in the left side flow chart can be SENKIN, PSR or other subroutines.

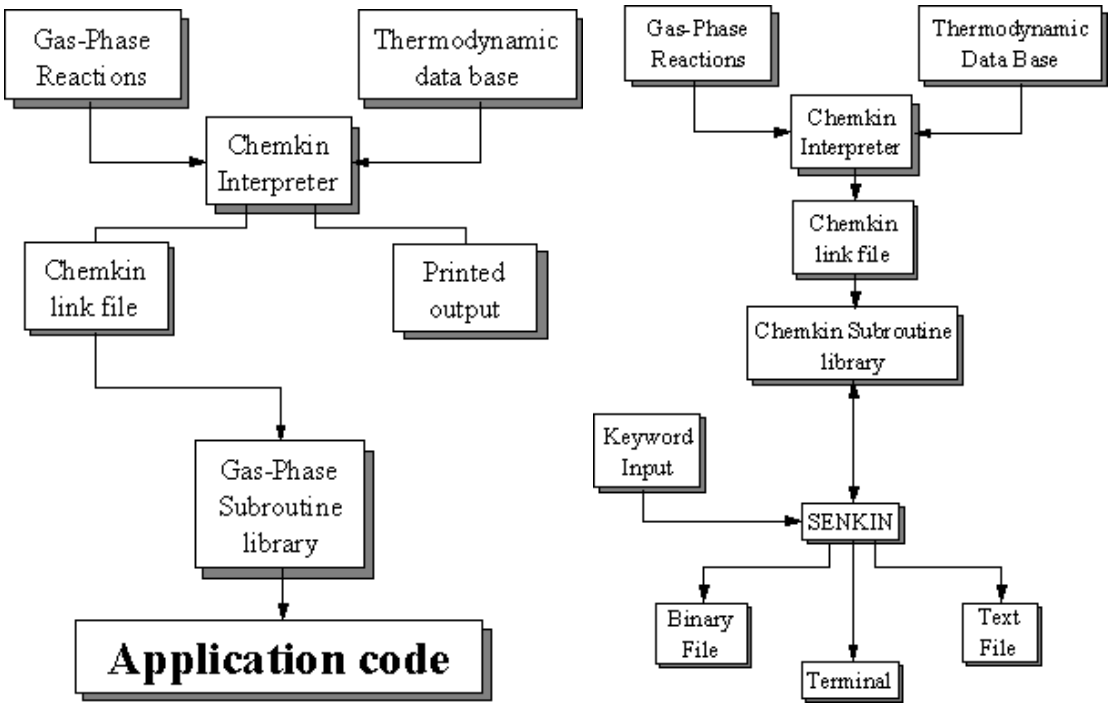

Figure 4-1. The Structure of Chemkin Package and the Relationship between SENKIN and Chemkin

4.2 Validation of Gas-Phase Mercury Oxidation Kinetics with Chemkin

An experiment was done by Ghorishi[7], in which simulated flue gas was passed through a 25.4cm (10in.) long constant diameter reactor, heated to specified temperature. Residence time of simulated flue gas in the reactor was 0.97s at 1027.15 K. After passage through the reactor, the flue gas was cooled rapidly to room temperature, with a quenching rate of 5990 K/s. Flue gas composition for Ghorishi experiments is shown in Table 4-1.

The Chemkin simulation results reported by Edwards et al.[8] show good agreement with the experiments done by Ghorishi. These results show that HCl decomposed to H and Cl, with the Cl atoms then reacting with Hg^0 to form $HgCl_2$. This simulation was conducted for 200, 100 and 50 ppmv HCl. Figure 4-2 shows the effects of HCl concentration on Hg conversion at 1027.15 K.

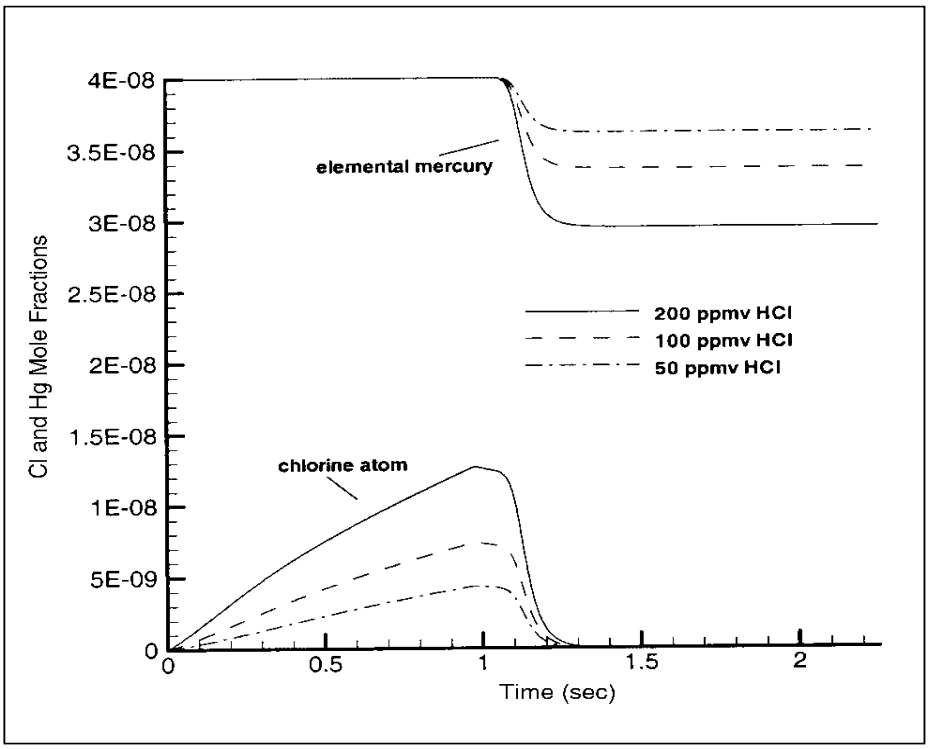

Figure 4-2. Cl and Hg Mole Fraction vs. Time Obtained in Chemkin Simulation By Edwards at 1027.15 K[9]

Species	Composition (mol fraction)
O_2	0.02
CO_2	0.05
HCl	50×10^{-6}
	100×10^{-6}
	200×10^{-6}
Hg	40×10^{-9}
N_2	balance

Table 4-1. Flue Gas Compositions For Ghorishi[8] Experiments

Similarly, the author of this report used the SENKIN sensitivity analyses to obtain the results illustrated in Figure 4-3.

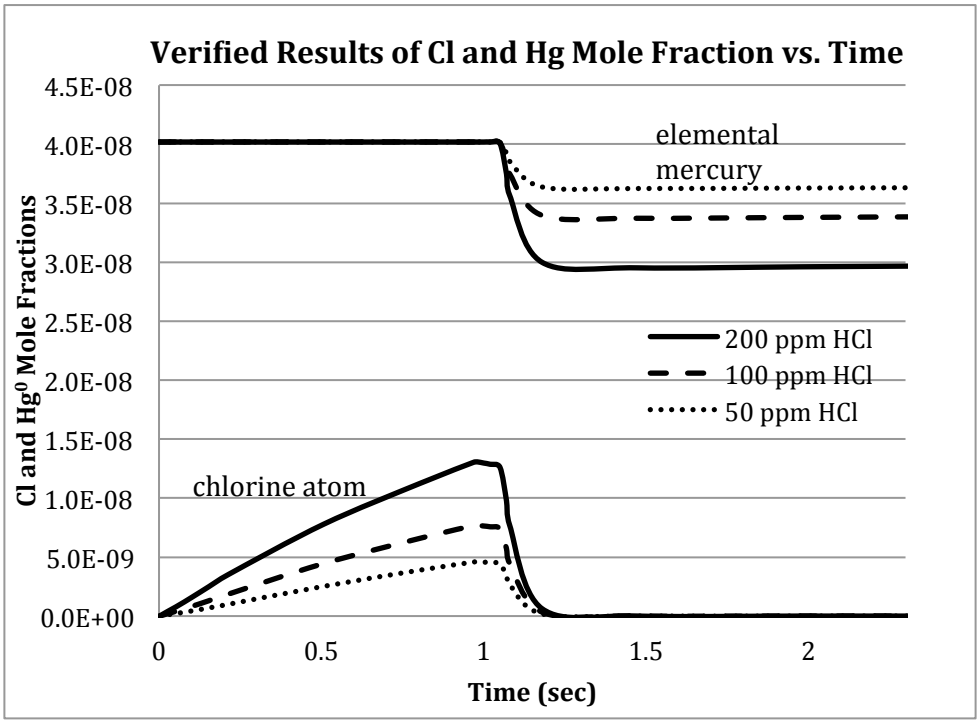

Figure 4-3. Results by the Author to Verify Results by Edwards Illustrated in Figure 4-2

Figure 4-3 shows the verified results obtained by the author with 200, 100 and 50 ppmv HCl concentrations at 1027.15 K. Figure 4-2 and Figure 4-3 show very good agreement between results by the author and by Edwards. This provides partial verification of the chemical kinetic calculations done by the author.

4.3 Inlet and Initial Conditions of Chemkin Simulation for Mercury Oxidation in CHX

Coal Creek station is a 1,100 MW station with two units burning a partially dried lignite coal from the adjacent Falkirk mine. Table 4-2 shows the mole fractions of all species used in kinetic modeling by the author. All of the species except for HCl and SO_3 are based on test data measured at the CHX inlet at approximate 210°F.

Flue Gas Composition	Coal Creek Station
Hg (ppbv)*	0.797
$HgCl_2$ (ppbv)*	0.373
HCl (ppmv)**	10
SO_2 (ppmv)*	898.9
SO_3 (ppmv)**	10
CO_2 (%)*	12.19
H_2O (%)*	12.9
O_2 (%)*	5.23
N_2 (%)*	~69.68(Balance)

Table 4-2. Flue Gas Composition For Mercury Oxidation Chemkin Modeling at the CHX Inlet

*Measured data by BARR Engineering
**Assumed data

The residence time is defined as the time it took for the flue gas to pass through each duct. The velocity of flue gas is calculated by flue gas mass flow rate over density of flue gas before it enters each duct.

The study of the elemental mercury oxidation was done in each individual heat exchanger. The moisture content and flue gas velocities at the inlet and outlet of each

heat exchanger were calculated. Then, the average velocity at each HTX was used to get the residence time and the cooling rate for the Chemkin simulations. Following are the calculation procedures and the results are shown in Table 4-3.

The gap of the tube bank in the duct:

$$A_{\text{gap}} = A_{\text{duct}} - A_{\text{bank}} = 0.201389 \text{ ft}^2$$

Flue gas velocity:

$$V_{\text{FGAS}} = \frac{\dot{m}_{\text{FGAS}}}{\rho_{\text{FGAS}} \cdot A_{\text{gap}}}$$

The average velocity in each HTX:

$$\bar{V}_{\text{FGAS,k}} = \frac{V_{\text{FGAS,inlet,k+1}} + V_{\text{FGAS,inlet,k}}}{2}, k = 1,2, \dots ,6$$

The flue gas residence time in each HTX:

$$t_{\text{R,k}} = \frac{L_{\text{Duct,k}}}{\bar{V}_{\text{FGAS,k}}}, k = 1,2, \dots ,6$$

$\Delta T/\Delta t$ in each HTX, using forward difference:

$$\frac{\Delta T}{\Delta t} = \frac{T_{\text{inlet,k+1}} - T_{\text{inlet,k}}}{t_{\text{R,k}}}, k = 1,2, \dots ,6$$

Note: when $k = 6, T_{\text{inlet,7}} = T_{\text{outlet,6}}, V_{\text{FGAS,inlet,7}} = V_{\text{FGAS,outlet,6}}$

	HTX1	HTX2	HTX3	HTX4	HTX5	HTX6	HTX6 Out
Inlet $y_{\mathrm{H2O,\%}}$	0.1287	0.1266	0.1212	0.1130	0.1010	0.0880	0.0773
$V_{\mathrm{FGAS,inlet,k}}$(ft/s)	16.79	16.66	16.38	15.77	15.05	14.41	13.95
Average Velocity $\bar{V}_{\mathrm{FGAS,k}}$ (ft/s)	16.73	16.52	16.07	15.41	14.73	14.18	-
Duct Length $L_{\mathrm{Duct,k}}$ (ft)	0.4275	0.5992	0.9433	1.2875	1.2875	1.2875	-
Flue Gas Residence Time $t_{\mathrm{R,k}}$ (s)	0.03	0.04	0.06	0.08	0.09	0.09	-
Inlet Temp $T_{\mathrm{inlet,k}}$ (K)	368.88	359.22	351.09	337.36	326.20	318.45	313.61
$\Delta T/\Delta t$ (K/s)	378.01	224.10	233.91	133.57	88.66	53.30	-

Table 4-3. Parameters in Each HTX in Low Temperature Test 3 on 9/27/2012

Table 4-2 and Table 4-3 give the initial and inlet conditions for Chemkin simulations to study elemental mercury oxidation.

4.4 Results of Chemkin Simulation for Mercury Oxidation in CHX

With the flue gas species shown in Table 4-2, Chemkin simulations in the CHX with the initial conditions shown in Table 4-3 were conducted to obtain the oxidation results shown in Table 4-4. In these simulations, it was assumed Hg^0 was reacted with HCl.

	CHX Inlet Conc. (ppbv)	CHX Outlet Conc. (ppbv)	Reduction (ppbv)	Reduction Rate %
10 ppmv HCl				
$HgCl_2$	0.373	0.3726575645	0.000342	0.091806
Hg^0	0.797	0.7962683081	0.000732	0.091806
100 ppmv HCl				
$HgCl_2$	0.373	0.3726240592	0.000376	0.100788
Hg^0	0.797	0.7961967162	0.000803	0.100788

Table 4-4. Hg and $HgCl_2$ Reduction Obtained by Chemkin Simulation with Same Inlet and Initial Conditions as Low Temperature Test 3 on 9/27 at temperature of 204°F

As the results presented in Table 4-4 show, the concentration of Hg^0 reduced by approximately 0.1% with 10 ppmv HCl. With the HCl concentration increased to 100 ppmv, the Hg^0 reduction rate was only ~0.101%. These results show that the rate of oxidation of Hg^0 is very insensitive to HCl concentration.

4.5 Analysis of Oxidation Results in CHX Obtained in Section 4.3

4.5.1 Dependence of Hg^0 oxidation on Cl concentration

As shown by Hall, Senior and others, the reaction between atomic Cl and Hg^0 dominates the Hg^0 oxidation rate. At temperatures below 725K, Figure 4-4 indicates all Hg is predicted to exist as $HgCl_2$ if equilibrium were to be achieved in the flue gas. At temperatures higher than 800K, the equilibrium model shows that HgO (g) can form slightly and mercury mainly exists as Hg^0.

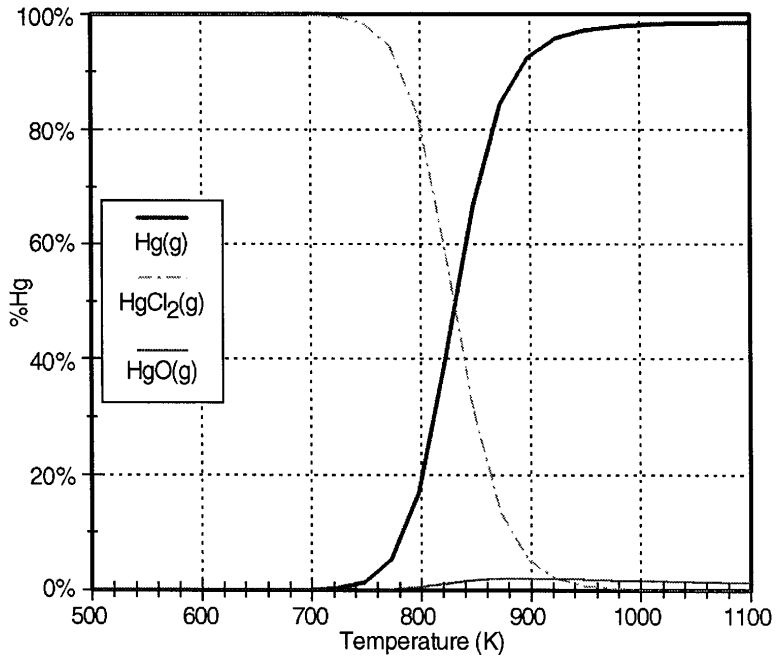

Figure 4-4. Equilibrium Mercury Speciation in Flue Gas as a Function of Temperature of Pittsburgh coal

A Chemkin simulation with adding 1 ppmv chlorine atoms was done by the author. The result shows that at 350K (170°F) in 1.5s, 45% Hg^0 would be converted to

$HgCl_2$ which is close to the measured results in Table 1 showing about 30% Hg^0 oxidation rate. Furthermore, with the same initial and inlet conditions, but instead adding 0.3 ppmv Cl atoms, the results of Hg^0 oxidation obtained by Chemkin were basically same as measured results. The next section of this report (section 4.5.2) deals with the effects of temperature on rate of formation of atomic chlorine.

4.5.2 Rate of Formation of Cl with Different Temperatures

Using the SENKIN code, calculations for the flue gas reaction $HCl \Leftrightarrow Cl + H$ at various temperatures were carried out to determine the effects of temperature on concentration.

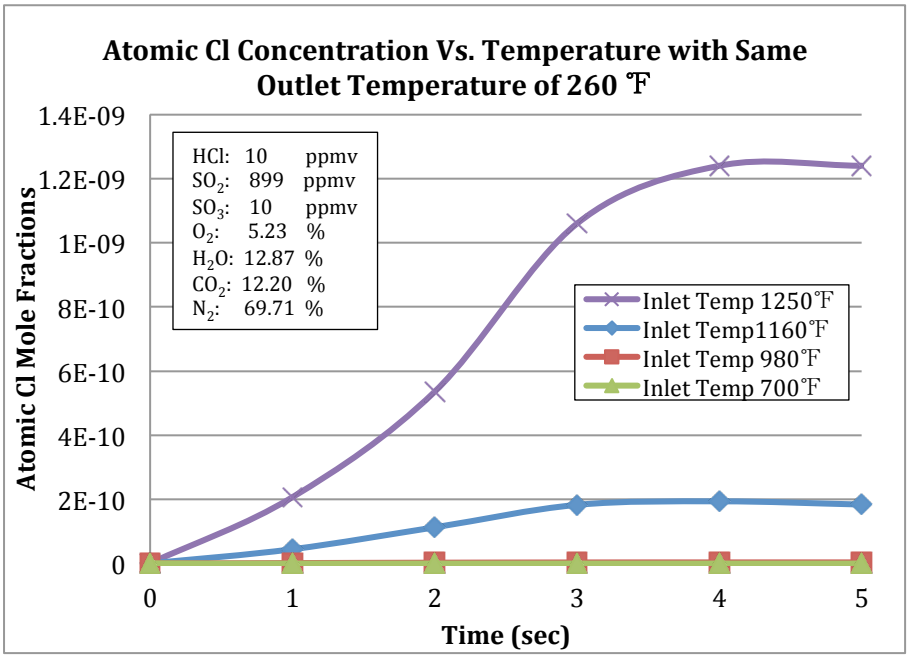

Figure 4-5. Atomic Cl Concentration Vs. Temperature with Four Different Inlet Temperatures and Same Outlet Temperature of 260°F

In these calculations, the gas contained all of the species shown in Table 4-2,

except Hg^0 and $HgCl_2$. Four different inlet temperatures: 1250°F, 1160°F, 980°F and 700°F and on outlet temperature of 260°F were assumed. The residence time is 5 seconds in all cases with derived cooling rates. The results are illustrated in Figure 4-5.

Figure 4-5 indicates the reaction $HCl \Leftrightarrow Cl + H$ goes to a state of equilibrium within 5 sec. The results also show that atomic Cl is formed at temperatures about 1000°F. With an inlet HCl concentration of 10 ppmv, 1.2 ppbv atomic Cl can be generated when the temperature goes up to 1250°F.

Chapter 5

Mercury Oxidation Kinetic Modeling from Furnace to the CHX

5.1 Kinetic Modeling Before ESP (Electrostatic Precipitator)

According to the mercury oxidation mechanism discussed previously, atomic chlorine plays a key role in elemental mercury oxidation and it thus is necessary to conduct an investigation of atomic Cl generating and transporting processes. A PSR (Perfectly Stirred Reactor) was used to estimate the Cl concentration in the flue gas at the furnace exit.

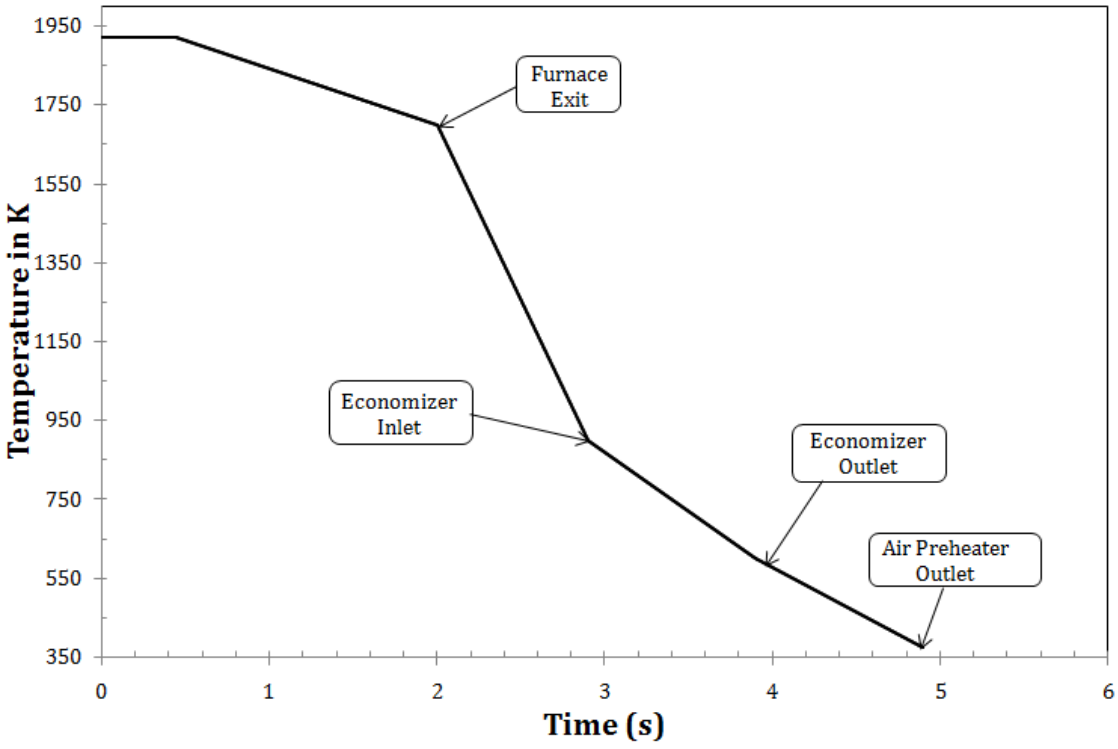

Figure 5-1. Time-temperature History for Pulverized Coal-fired Boiler

It is assumed that the time-temperature history presented in Figure 5-1 is similar for most power plants. A typical composition of flue gas at furnace exit is shown in Table 5-1 as below.

Species	Mole Fraction	Species	Mole Fraction
Hg (ppbv)**	4.0	**CO_2 (%)***	15.6
HCl (ppmv)**	10	**H_2O (%)***	16.51
SO_2 (ppmv)*	1151	**O_2 (%)****	0.75
SO_3 (ppmv)**	12.8	**N_2 (%)***	~67.02(Balance)

Table 5-1. Composition of Flue Gas at Furnace Exit

*Estimated from measured data by BARR Engineering

**Assumed values

Using the species shown in Table 5-1 with a HCl concentration of 10 ppmv at the temperature of 1700K, with a furnace volume of 500m^3 and in the residence time of 0.5s, the equilibrium concentrations of all possible species are presented in Table 5-2.

At the temperature of 1700K, the equilibrium concentration of Hg^0 was nearly same as the inlet Hg concentration. Approximate 0.3% Hg^0 converted to HgO and a very slight amount of Hg^0 was oxidized to HgCl or $HgCl_2$. With 10 ppmv HCl, atomic Cl was generated relatively significantly at this temperature about 0.2 ppmv.

HGCL2	=	5.03E-20	HGO	=	1.06E-11	HG	=	3.99E-09
HGCL	=	6.62E-16	CL2	=	9.22E-13	CLO	=	4.07E-11
HCL	=	9.82E-06	CL	=	1.77E-07	CLO2	=	0.00E+00
COCL	=	0.00E+00	HOCL	=	3.66E-10	NOCL	=	3.25E-16
O	=	3.66E-06	OH	=	2.03E-04	O2	=	7.53E-03
O3	=	0.00E+00	H	=	8.38E-07	H2	=	3.60E-05
H2O	=	1.65E-01	H2O2	=	7.83E-09	HO2	=	8.45E-08
HCO	=	0.00E+00	CO	=	1.15E-04	CO2	=	1.56E-01
HNO	=	1.94E-13	HONO	=	6.62E-13	N2	=	6.70E-01
N2O	=	2.54E-08	NO	=	7.35E-08	NO2	=	4.24E-11
NO3	=	0.00E+00	S	=	2.18E-12	SO	=	7.63E-08
SO2	=	1.16E-03	SO3	=	1.56E-06			

Table 5-2. Equilibrium Composition of Flue Gas at Furnace Exit with 10 ppmv HCl at 1700K

At the temperature of 1700K (2600°F) and in the furnace volume of ~ 200-500m^3, the simulation shows the concentration of atomic Cl would not change significantly as residence time increased. Therefore, all of the reactions are in equilibrium.

Generally, air leaking into the flue gas ducts occurs downstream of the boiler which was considered in the kinetic calculations. Therefore, species concentrations except O_2 and N_2 decreased due to dilution. With typical O_2 concentrations of 0.75% at furnace exit, 3.5% at economizer inlet, 4.25% at air preheater and 5.23% measured at CHX inlet, the amount of leaking air can be determined.

Generally, there will be a temperature drop from 1700K to 900K (2600°F to 1160°F) within 0.9s from furnace exit to economizer inlet. With these inlet and outlet temperatures and cooling rates, new species concentrations can be obtained by SENKIN kinetic modeling using the species shown in Table 5-2.

HGCL2	= 2.75E-15	HGO	= 1.90E-11	HG	= 3.44E-09
HGCL	= 2.09E-15	CL2	= 1.25E-11	CLO	= 7.22E-12
HCL	= 8.62E-06	CL	= 1.86E-08	CLO2	= 0.00E+00
COCL	= 0.00E+00	HOCL	= 1.80E-10	NOCL	= 5.71E-14
O	= 5.01E-10	OH	= 3.09E-07	O2	= 3.50E-02
O3	= 0.00E+00	H	= 1.13E-11	H2	= 1.89E-08
H2O	= 1.43E-01	H2O2	= 1.05E-08	HO2	= 1.38E-09
HCO	= 6.44E-20	CO	= 1.39E-07	CO2	= 1.35E-01
HNO	= 1.12E-14	HONO	= 3.12E-13	N2	= 6.86E-01
N2O	= 1.51E-08	NO	= 1.26E-07	NO2	= 1.28E-09
NO3	= 0.00E+00	S	= 5.12E-22	SO	= 4.64E-13
SO2	= 9.92E-04	SO3	= 1.18E-05		

Table 5-3. Composition of Flue Gas at Economizer Inlet with 10 ppmv HCl at 900K

In Table 5-3, compared to species concentrations shown in Table 5-2, Hg^0 concentration still did not change significantly but ~0.019 ppbv Hg^0 was oxidized to HgO which verified HgO can form slightly at temperatures higher than ~800K. The concentration of atomic Cl became one-tenth of that at the furnace exit at the temperature of 1700K because atomic Cl will combine to form HCl and minor amounts of Cl_2.

A SENKIN kinetic modeling was then performed from the economizer inlet to ESP inlet with the inlet species concentrations shown in Table 5-3. Table 5-4 presents the concentrations of all species at the ESP inlet.

HGCL2	= 8.51E-10	HGO	= 1.82E-11	HG	= 2.09E-09
HGCL	= 3.53E-10	CL2	= 1.12E-09	CLO	= 5.34E-12
HCL	= 8.25E-06	CL	= 3.17E-09	CLO2	= 0.00E+00
COCL	= 0.00E+00	HOCL	= 9.10E-09	NOCL	= 8.49E-13
O	= 8.48E-19	OH	= 4.80E-15	O2	= 4.25E-02
O3	= 0.00E+00	H	= 1.88E-19	H2	= 7.09E-09
H2O	= 1.37E-01	H2O2	= 4.39E-09	HO2	= 9.58E-12
HCO	= 3.71E-28	CO	= 1.13E-07	CO2	= 1.29E-01
HNO	= 8.82E-18	HONO	= 1.20E-18	N2	= 6.91E-01
N2O	= 1.44E-08	NO	= 1.17E-07	NO2	= 5.10E-09
NO3	= 0.00E+00	S	= 1.91E-39	SO	= 9.76E-27
SO2	= 9.50E-04	SO3	= 1.14E-05		

Table 5-4. Composition of Flue Gas at the ESP Inlet with 10 ppmv HCl at 375K

After the flue gas passed through economizer and air preheater, with the air leakage, Hg^0 concentration decreased to about 50% at the ESP inlet. However, atomic Cl was still in ppbv level as expected.

Figure 5-2 indicates atomic Cl has a concentration up to 1×10^{-6} at furnace exit. The mercury oxidation rate limiting reaction HCl + OH = Cl + H_2O occurs and temperature drops before flue gas enters economizer, which make atomic Cl concentration decrease significantly. In economizer and APH, the concentration of atomic Cl would generally decrease due to Hg^0 oxidation and recombination of Cl with H. Within the range of furnace exit HCl concentrations from 0.01 ppbv to less than 1 ppbv, the atomic Cl essentially does not react with Hg^0 due to very low concentration.

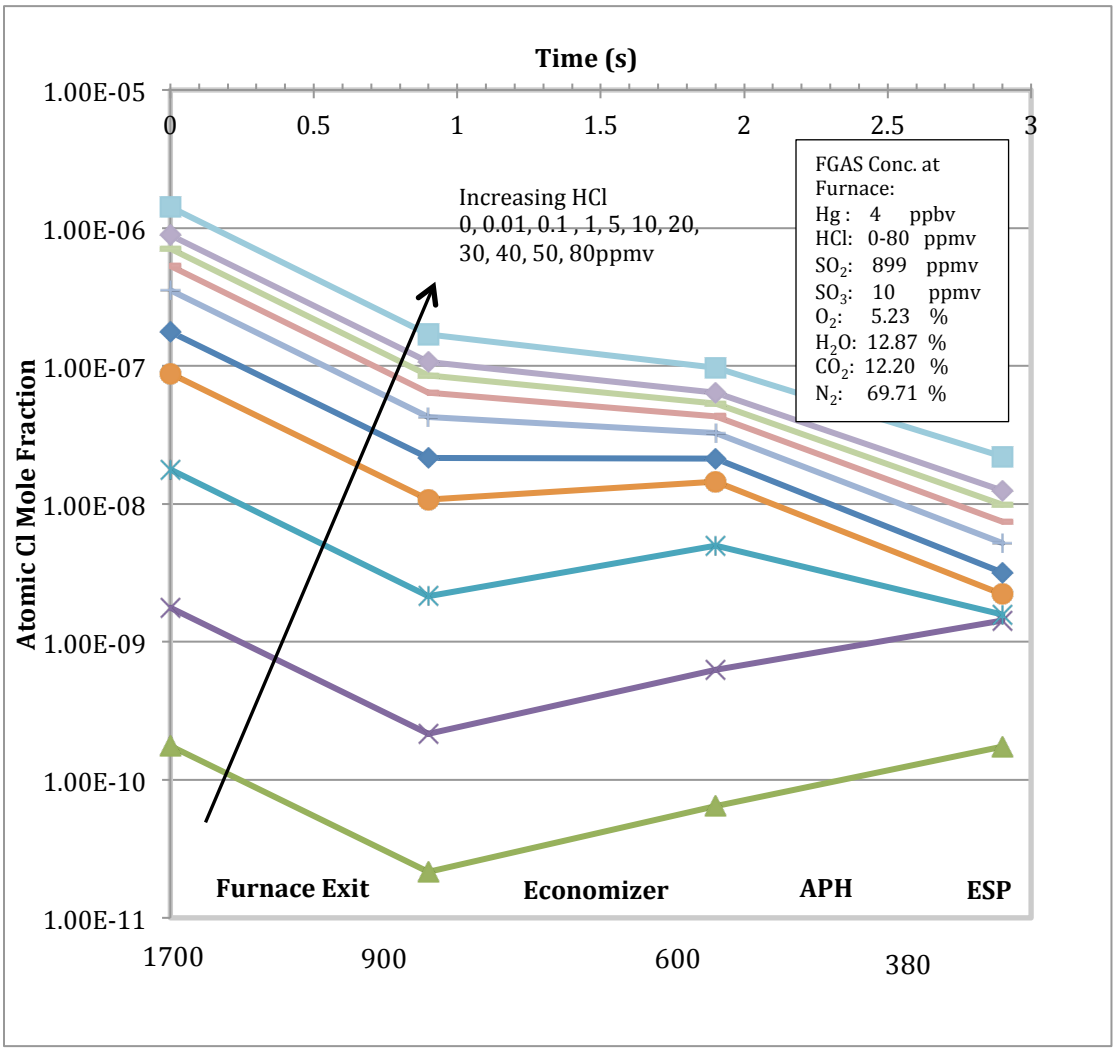

Figure 5-2. Atomic Cl Concentration vs. Time with Different HCl Concentrations

5.2 Mercury Behavior for the Flue Gas Across ESP

In the tests done at Great River Energy on 9/27/2012 and 9/28/2012, the flue gas passed through the ESP before it entered the CHX. The ESP is the most commonly used APCD in coal-fired power plant and it is usually located downstream of the air preheater at about 160°C (320°F) which provides optimal resistivity of the coal-ash particles.

Wang et al.[9] measured the characterization of mercury emissions and their behavior in six typical coal-fired power plants in China and concluded ESPs can capture nearly all particulate mercury (Hg_p). Table 5-5 shows the concentrations of different forms of mercury in the flue gas at APCDs of six different coal-fired power plants in China.

		Plant 1	Plant 2	Plant 3	Plant 4	Plant 5	Plant 6
Before SCR	Total Hg						1.92±0.05
($\mu g/m^3$)	Hg^{2+}						0.15±0.04
	Hg^0						1.55±0.12
	Hg_p						0.22±0.02
Before ESP	Total Hg	20.77±2.17	15.06±1.99	27.15±0.46	3.13±0.13	26.93±2.33	1.89±0.13
($\mu g/m^3$)	Hg^{2+}	11.42±0.74	4.64±0.83	22.22±0.35	0.42±0.11	23.73±1.83	0.40±0.10
	Hg^0	6.00±0.66	7.05±0.32	2.11±0.32	2.48±0.26	2.78±0.40	1.02±0.07
	Hg_p	3.36±0.17	3.37±0.53	2.82±0.36	0.23±0.04	0.42±0.10	0.47±0.02
After ESP	Total Hg	13.20±1.89	8.07±1.15	24.35±0.64	2.94±0.11	21.96±4.13	1.44±0.04
($\mu g/m^3$)	Hg^{2+}	8.92±1.24	3.99±0.39	17.90±0.58	0.42±0.06	18.36±3.64	0.44±0.03
	Hg^0	4.27±0.74	4.08±0.63	6.44±0.55	2.50±0.14	3.58±0.57	1.00±0.03
	Hg_p	0.01±0.00	0.00±0.00	0.00±0.00	0.02±0.00	0.02±0.00	0.00±0.00
After FGD	Total Hg	6.69±1.24	4.53±0.68	5.06±0.43	2.27±0.19		1.22±0.12
($\mu g/m^3$)	Hg^{2+}	1.66±0.64	0.84±0.20	0.45±0.09	0.14±0.03		0.13±0.02
	Hg^0	5.03±1.05	3.70±0.40	4.61±0.46	2.13±0.20		1.08±0.11
	Hg_p	0.00±0.00	0.00±0.00	0.00±0.00	0.00±0.00		0.00±0.00
After FF	Total Hg					9.16±1.69	
($\mu g/m^3$)	Hg^{2+}					3.04±0.64	
	Hg^0					6.11±1.09	
	Hg_p					0.01±0.00	

Table 5-5. Concentrations of Different Forms of Mercury in the Flue Gas at APCDs of Six Coal-fired Power Plants in China[10]

Table 5-5 indicates the flue gas Hg^0 and Hg^{2+} concentrations after ESP could be considered same as those before ESP with the uncertainties of measurement. In all these simulations, it was assumed that the Hg^0 and Hg^{2+} would convert to Hg_p downstream of the boiler before flue gas entered ESP and all Hg_p would be removed by ESP.

In order to compare the simulated Hg^0 oxidation results with measured results in the tests done at Great River Energy, the Hg^0 and Hg^{2+} concentrations are assumed to be the same as measured values in the tests at Great River Energy on 9/27/2012 and 9/28/2012.

The Hg^0 and Hg^{2+} concentrations before and after ESP are shown in Table 5-6 with 4 ppbv Hg at the furnace exit.

4 ppmv Hg at Furnace Exit		
Before ESP (ppbv)	Total Hg	3.310*
	Oxidized Hg	1.223*
	Hg^0	2.087*
After ESP (ppbv)	Total Hg	1.170**
	Oxidized Hg	0.373**
	Hg^0	0.797**

Table 5-6. Flue Gas Concentrations of Different Forms of Mercury with 10 ppmv HCl Before and After ESP with 4 ppbv Hg at Furnace Exit

*Simulated values based on 4 ppbv Hg^0 at furnace exit

**Measured data

5.3 Kinetic Modeling in the CHX

The SENKEN analysis was performed by same steps in section 4.3 with species concentrations shown in Table 5-4, except it was assumed particulate mercury was removed by the ESP shown in Table 5-6.

Table 5-7 shows the flue gas compositions at different locations downstream of the furnace.

Flue Gas Composition	Furnace	Furnace Exit	Economizer Inlet	APH Inlet	ESP Inlet	CHX Inlet
Hg^0 (ppbv)	4**	3.99	3.44	3.28	2.09	0.797*
Oxidized Hg (ppbv)	0	0.0106	0.0220	0.0217	1.22	0.373*
HCl (ppmv)	10**	9.82	8.62	8.25	8.25	7.80
SO_2 (ppmv)	1151	1160	992	949	949	897*
SO_3 (ppmv)	12.8**	1.56	11.8	11.4	11.4	10.7**
CO_2 (%)	15.6	15.6	13.5	12.9	12.9	12.2*
H_2O (%)	16.51	16.51	14.27	13.66	13.66	12.91*
O_2 (%)	0.75	0.75	3.5	4.25	4.25	5.23*
N_2 (%) Balance	67.02	67.02	68.63	69.08	69.08	69.63*

Table 5-7. Flue Gas Composition Downstream of the Boiler with Air Leaking into the Flue Gas Ducts

*Measured values by BARR Engineering
**Assumed values
Others are calculated values

The predicted changes in Hg^0 are due to oxidation of the Hg^0. Change in most other parameters are assumed to be primarily due to air leakage. At the furnace temperature up to 1900K, SO_3 will decompose to SO_2 which makes assumed SO_3 concentration at furnace exit decrease to 1.56 ppmv. With flue gas flow downstream of

the furnace, SO_3 will reform and stay stable with temperature going down. However, the temporary change of SO_2 and SO_3 in furnace would not affect the mercury oxidation results.

Figure 5-3 shows the mole fractions of different forms of mercury vs. time and temperature downstream of the furnace exit.

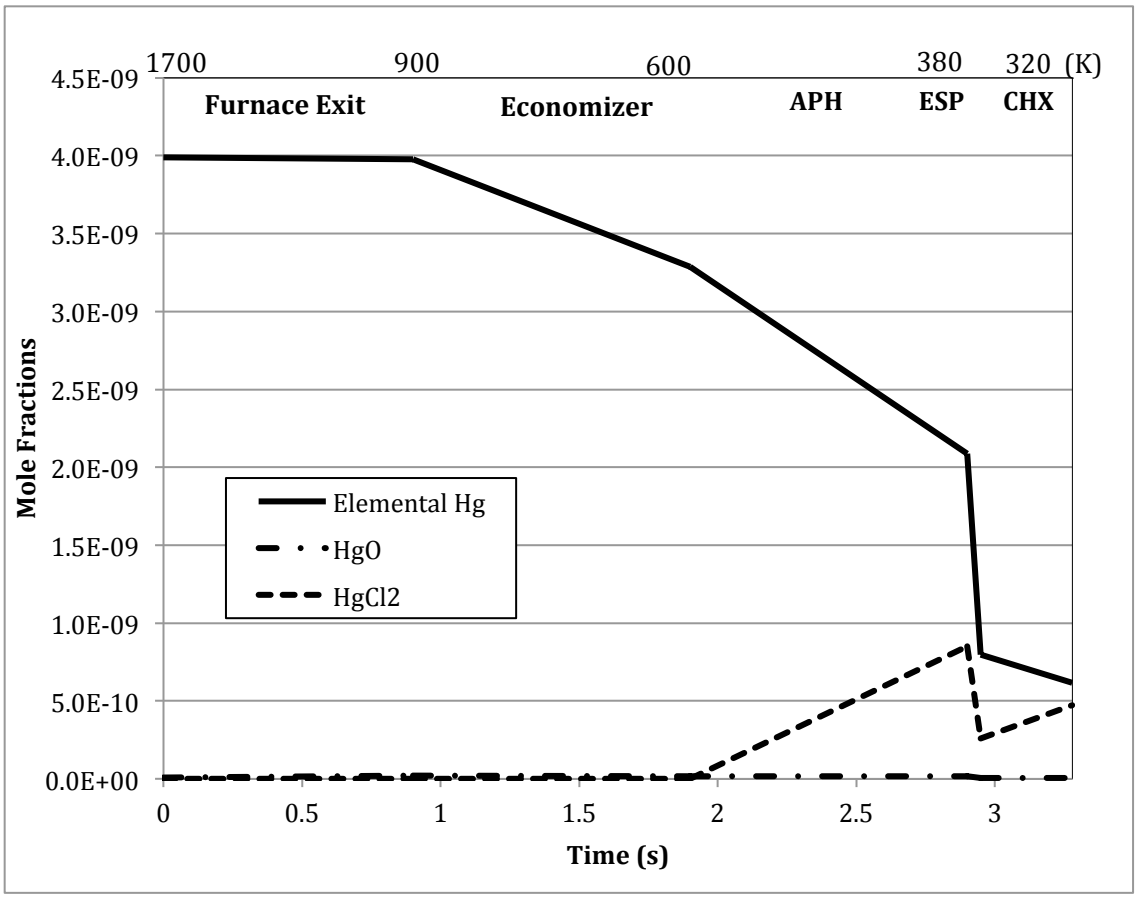

Figure 5-3. Hg^0, HgO and $HgCl_2$ Concentrations vs. Time with 10 ppmv HCl

In Figure 5-3, Hg^0 decreases and $HgCl_2$ forms significantly after the flue gas enters air preheater. These results indicate atomic Cl would react with Hg^0 at the temperature range of 600K to 300K (620°F to 80°F) with proper cooling rate. HgO

mainly formed in the furnace at the temperature higher than 1500K. Figure 11 also indicates the Hg^0 is oxidized in this case.

The comparison of mercury oxidation results between simulation and test in the CHX with total mercury of 4 ppbv at furnace exit is shown in Table 5-8.

	Simulation	Test		Simulation	Test
CHX Inlet Hg^0 Conc. (ppbv)	0.797	0.797	**CHX Inlet Temperature (°F)**	206.11	204.31
CHX Outlet Hg^0 Conc. (ppbv)	0.617	0.516	**CHX outlet Temperature (°F)**	102.40	104.83
Hg^0 Reduction (ppbv)	0.180	0.281	**Hg^0 Conc. At Furnace Exit (ppbv)**	4.00	-
Hg^0 Reduction Rate %	22.58	35.25	**HCl Conc. In Flue gas (ppmv)**	10.00	-

Table 5-8. Mercury Oxidation in CHX of Simulation and Test with 10 ppmv HCl

Table 5-8 compares the predicted elemental Hg oxidation results in the CHX with data from low temperature test with 10 ppmv HCl. This comparison shows a not very good agreement between simulation and test. However, the rough assumption of HCl concentration in the simulation and uncertainties of measurement in the test may cause this disagreement.

In the next section, how HCl concentration in flue gas affects Hg^0 oxidation in the CHX is investigated.

Chapter 6

Comparison and Discussion on Mercury Oxidation Results

6.1 Comparison of Simulation and Measured Results

Because of the lack of data on HCl concentration and the disagreement between the tests and simulations with 10 ppmv HCl in flue gas, the sensitivity analysis of HCl concentration in Hg^0 oxidation was carried out with HCl concentrations in flue gas from 0.01 ppmv to 80 ppmv. Total mercury of 4 ppbv at furnace exit was assumed for the following simulation and analysis. Table 6-1 predicts Hg^0 oxidation simulation results in the CHX with different flue gas HCl concentrations from 0.01 to 80 ppmv.

Furnace Exit HCl Conc. (ppmv)	CHX Inlet Atomic Cl Conc. (ppbv)	CHX Outlet Atomic Cl Conc. (ppbv)	CHX Inlet Hg^0 Conc. (ppbv)	CHX Outlet Hg^0 Conc. (ppbv)	Hg^0 Conc. Reduction (ppbv)	Hg^0 Reduction Rate %
0.01	0.165	0.08	0.797	0.79657	0.00043	0.05
0.1	1.35	1.16	0.797	0.79657	0.00043	0.05
1	1.49	1.08	0.797	0.71094	0.08606	10.80
5	2.09	1.54	0.797	0.67142	0.12558	15.76
10	2.99	2.22	0.797	0.61688	0.18012	22.60
20	4.90	3.64	0.797	0.54722	0.24978	31.34
30	7.02	5.22	0.797	0.51706	0.27994	35.12
40	9.31	6.85	0.797	0.51509	0.28191	35.37
50	11.79	8.55	0.797	0.53058	0.26642	33.43
80	20.83	14.51	0.797	0.59937	0.19763	24.80
Low Temp Test	**-**	**-**	***0.797***	***0.516***	***0.281***	***35.25***

Table 6-1. Hg^0 Oxidation Results in the CHX with Different HCl Concentrations

Table 6-1 presents the concentrations of HCl used in simulations. Agreement with test results occur in the range of HCl at the furnace exit of less than 20 ppmv to greater than 50 ppmv.

Figure 6-1 illustrates Hg^0 concentrations vs. time with different concentrations of HCl from the furnace exit to the CHX. It shows significant Hg^0 oxidation would occur at APH and CHX.

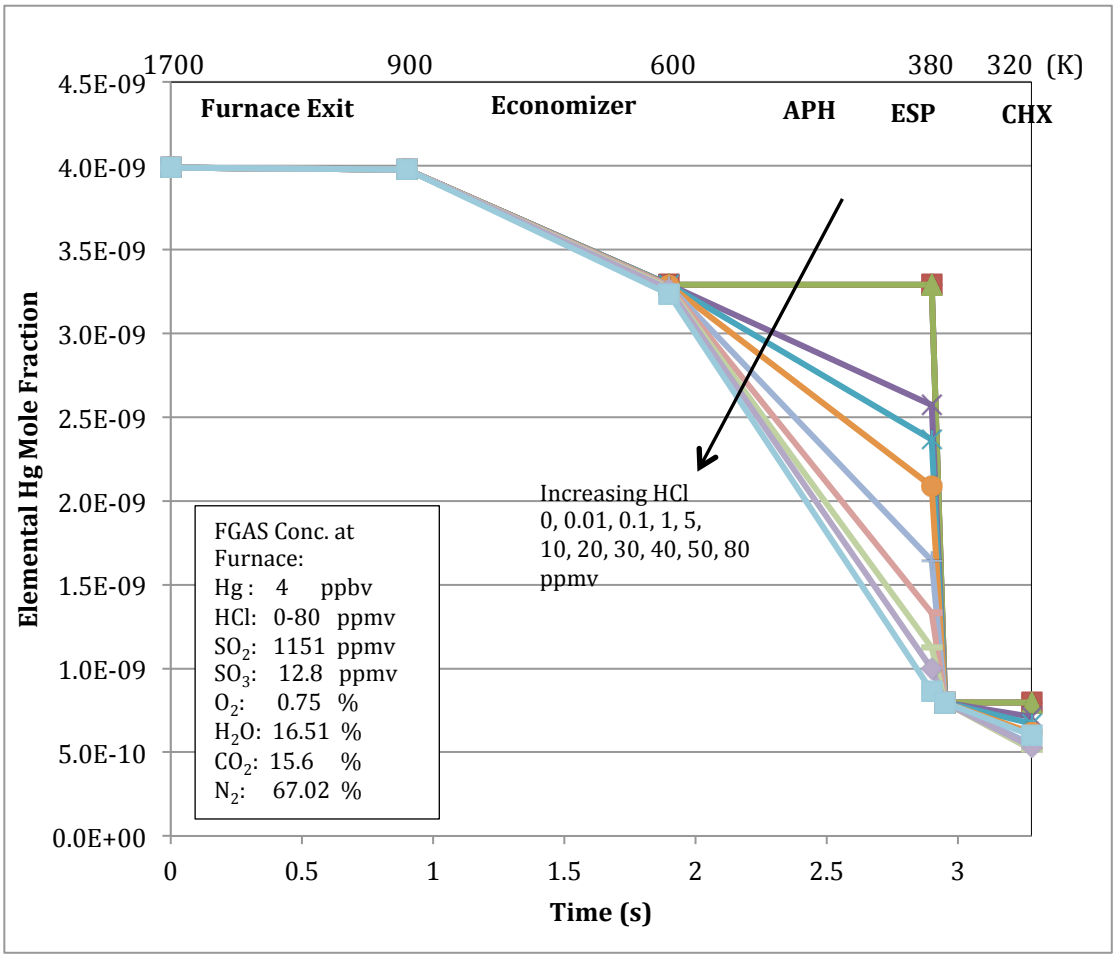

Figure 6-1. Hg^0 Concentrations vs. Time with Different HCl Concentrations at the Furnace Exit

Figure 6-1 indicates that a higher HCl concentration in the furnace will cause more Hg^0 to be oxidized in the APH. However, the peak value of Hg^0 oxidation rate in the CHX is 36% when HCl concentration is ~40 ppmv at the furnace exit. The predicted Hg^0 oxidation rate decreases as the HCl concentration is more than 40 ppmv which is shown in Figure 6-2. In the range of HCl concentration of 20-50 ppmv, the predicted mercury oxidation rate does not increase with HCl concentration increase.

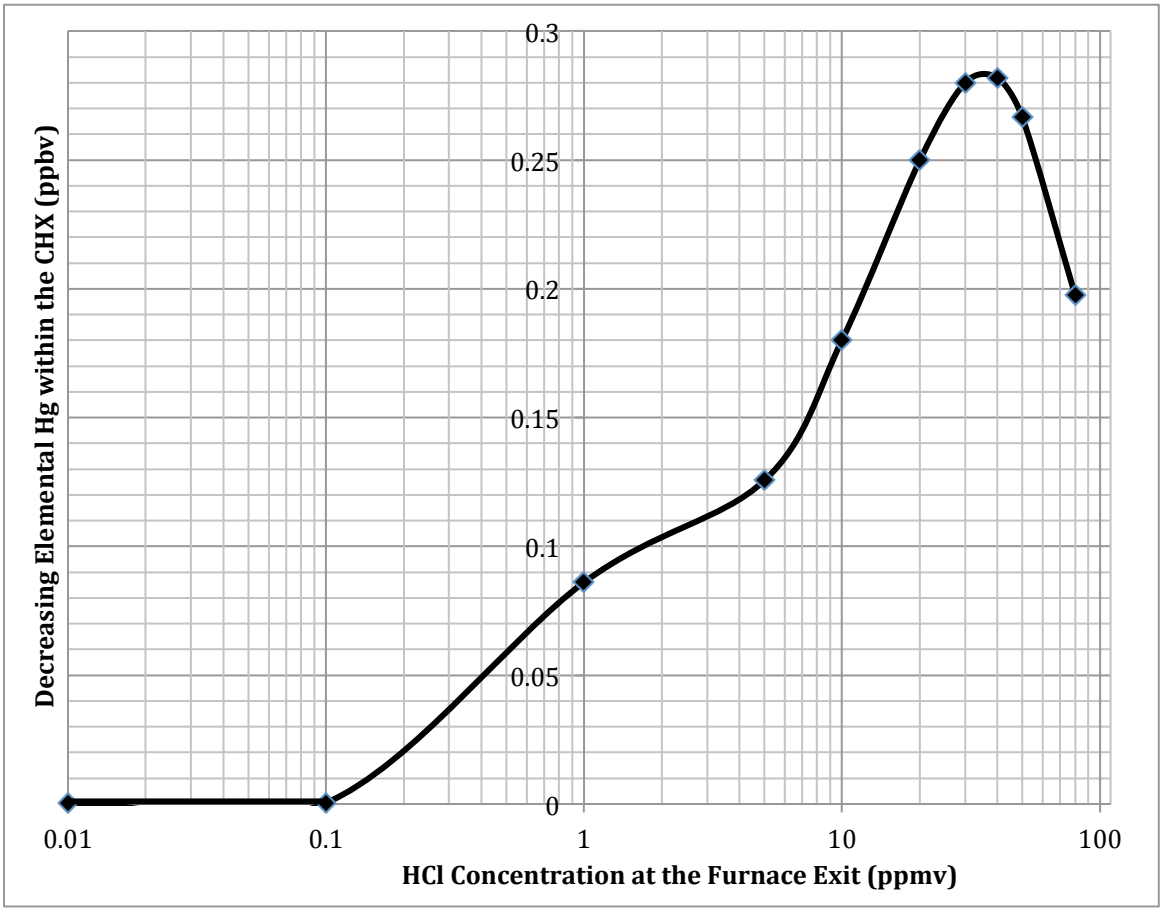

Figure 6-2. Hg^0 Concentrations vs. Time with Different HCl Concentrations

Furthermore, the simulation with high temperature conditions which are same as the test done on 9/28/2012 at Great River Energy was carried out. Table 6-2 shows the comparison of predicted Hg^0 oxidation results between simulation with 40 ppmv HCl in the flue gas at the furnace exit and test in low and high temperature cases. The low temperature Hg^0 oxidation has very good agreement between simulation and test. However, in the high temperature case, using different inlet Hg^0 concentration with low temperature case, the Hg^0 oxidation rate is a little bit higher in simulation than in the test.

	CHX Inlet Atomic Cl Conc. (ppbv)	CHX Inlet Hg^0 Conc. (ppbv)	Hg^0 Conc. Reduction (ppbv)	Hg^0 Reduction Rate %
Low Temp Simulation	0.797	0.515	0.282	35.37
Low Temp Test	***0.797***	***0.516***	***0.281***	***35.25***
High Temp Simulation	0.983	0.588	0.395	40.18
High Temp Test	***0.983***	***0.663***	***0.320***	***32.55***

Table 6-2. Comparison of Hg^0 Oxidation Results between Simulation and Test with 40 ppmv HCl in Low and High Temperature Cases Respectively in the CHX

It is assumed that the simulations have same flue gas compositions with the tests on 9/27/2012 and 9/28/2012. However, the CHX inlet Hg^0 concentrations are different between these two tests. These different CHX inlet Hg^0 concentrations and the uncertainties of measurement might cause the disagreement between simulation and test in the high temperature case.

6.2 Effects of Flue Gas Temperature in the CHX on Hg^0 Oxidation

6.2.1 Flue Gas Temperature Prediction in the CHX

An analytical model of heat and mass transfer processes in the CHX was developed by the ERC at Lehigh University. With same conditions of the tests done at Great River Energy except the CHX inlet cooling water temperature, using the numerical simulation software, the flue gas temperature profiles in the CHX were predicted. Figure 6-3 presents predicted temperature profiles through heat exchanger 1 (HX1) to HX6 with assumed cooling water temperatures from 35°F to 100°F.

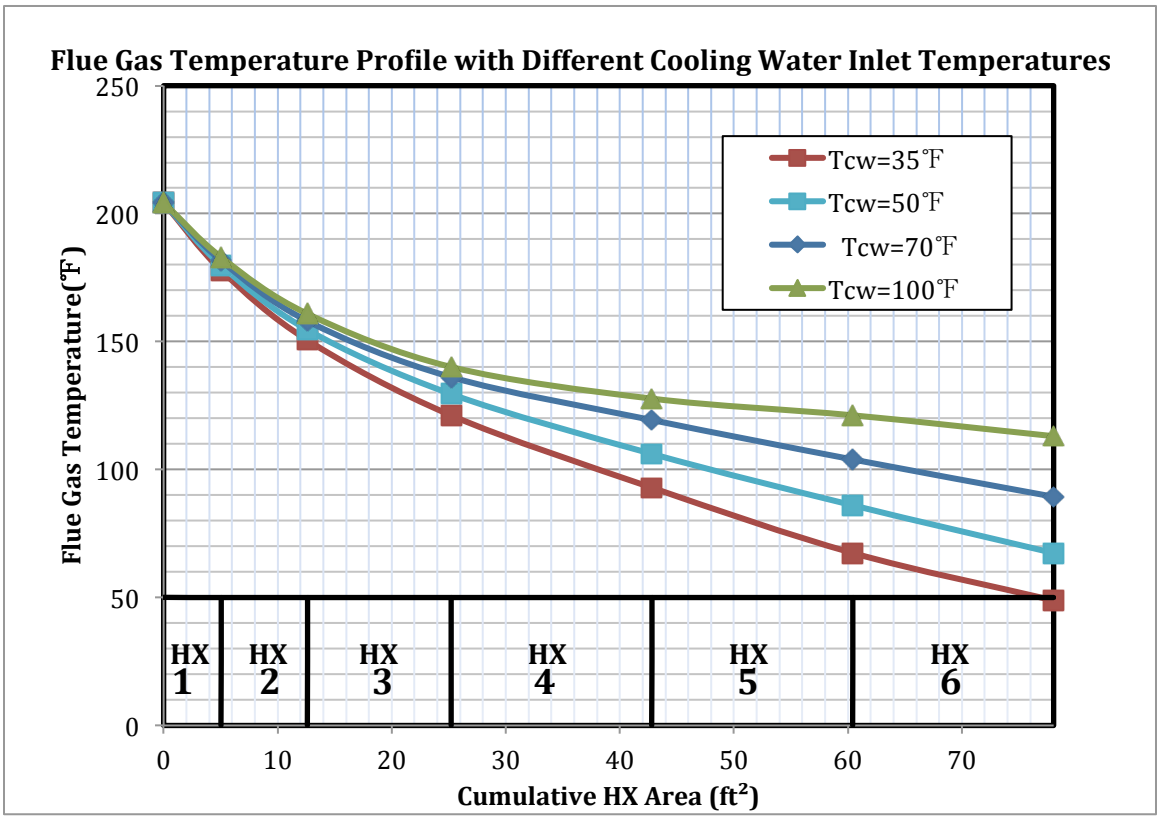

Figure 6-3. Predicted Flue Gas Temperature Profile with Different Inlet Cooling Water Temperatures of the CHX

The different CHX inlet cooling water temperatures would lead to different heat and mass transfer processes in the CHX. The moisture contents of flue gas are also significantly different due to condensed water formed though the six sections of the CHX. Figure 6-4 shows the dew point temperatures (T_{dew}) and the tube wall temperatures (T_{sc}) at different CHX inlet cooling water temperatures. The low CHX inlet cooling water temperature makes condensed water form immediately when flue gas enters into the CHX due to the low surface contact temperature on tubes. On the contrary, moisture content does not change at the first three sections when the CHX inlet cooling water temperature up to 100°F.

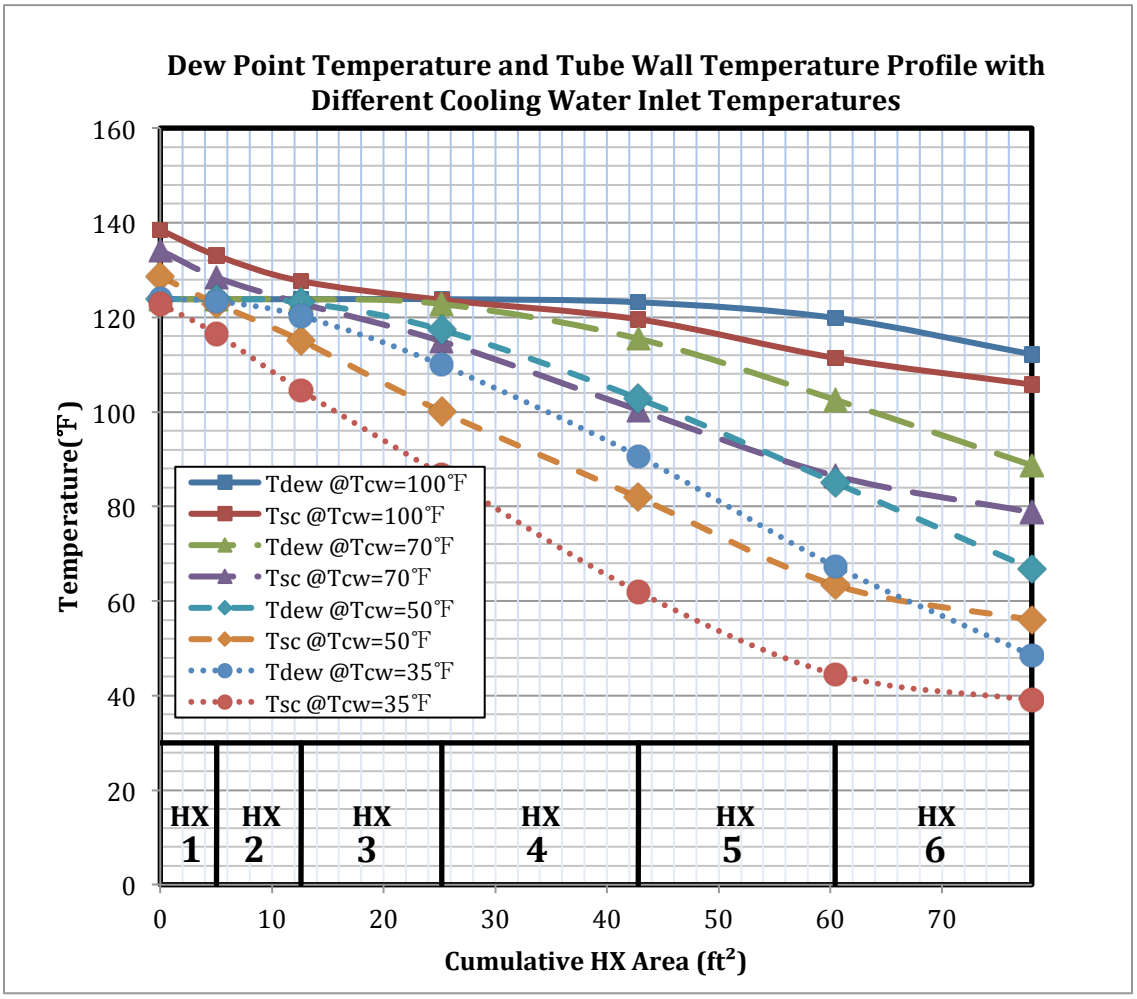

Figure 6-4. Dew Point Temperature and Tube Wall Temperature Profile with Different Inlet Cooling Water Temperatures of the CHX

The condensed water forms and leaves the CHX at each individual section. This causes the flue gas moisture content to decrease through the six sections of the CHX which is shown in Figure 6-5.

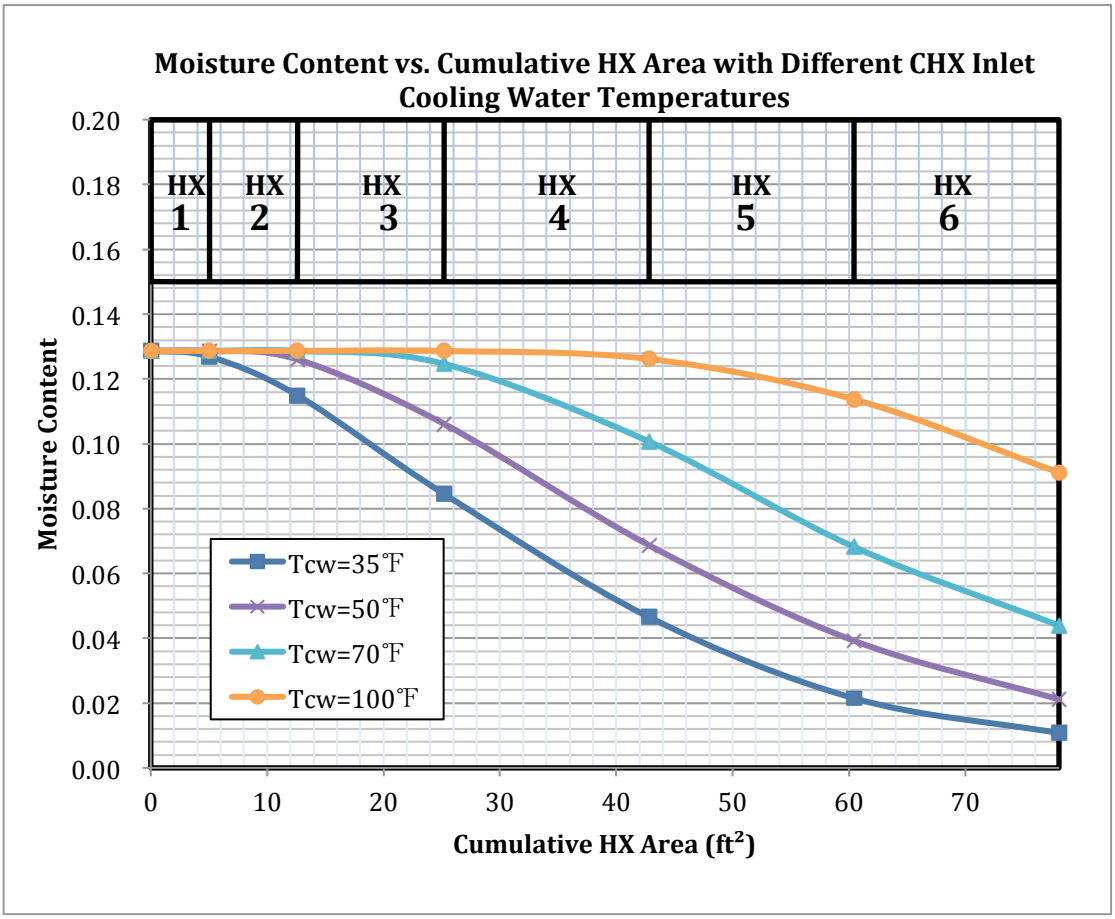

Figure 6-5. Moisture Content with Different Inlet Cooling Water Temperatures of the CHX

Figure 6-5 illustrates the moisture content of flue gas would be significantly lower with inlet cooling water temperature of 35°F. Meanwhile, large amount of condensed water forms and captures oxidized mercury in the CHX.

6.2.2 Hg^0 Oxidation Simulation Results with Different Flue Gas Temperatures in the CHX

With temperature profiles and moisture content of flue gas profiles in section 6.2.1, the Hg^0 oxidation modeling in the CHX was carried out to investigate the effects of flue gas temperature and moisture concentration on Hg^0 oxidation rate. Table 6-3 shows the Hg^0 reduction rate is up to 37.36% when the CHX inlet cooling water temperature is 35°F with the furnace exit HCl concentration of 20 ppmv. The Hg^0 reduction rate increases from 30.91% to 37.36 with CHX inlet cooling water temperature decreases from 100°F to 35°F with the furnace exit HCl concentration of 20 ppmv.

Inlet Cooling Water Temp (°F)	Furnace Exit HCl Conc. (ppmv)	CHX Inlet Atomic Cl Conc. (ppbv)	CHX Outlet Atomic Cl Conc. (ppbv)	CHX Inlet Hg^0 Conc. (ppbv)	CHX Outlet Hg^0 Conc. (ppbv)	Hg^0 Conc. Reduction (ppbv)	Hg^0 Reduction Rate %
35	40	9.3	6.613	0.797	0.46033	0.33667	42.24
35	20	4.9	3.523	0.797	0.49927	0.29773	37.36
50	20	4.9	3.555	0.797	0.51479	0.28221	35.41
70	20	4.9	3.614	0.797	0.53331	0.26369	33.09
100	20	4.9	3.673	0.797	0.55063	0.24637	30.91

Table 6-3. Hg^0 Oxidation Results in the CHX with Different Inlet Cooling Water Temperatures of the CHX

With the HCl concentration of 20 ppmv, the peak value of Hg^0 oxidation rate which is 37.36% can be obtained at the CHX inlet cooling water temperature of 35°F.

Using same conditions except increasing the HCl concentration to 40 ppmv, the predicted Hg^0 oxidation rate goes up to 42.24%.

Simulations conducted by Li[11] suggest a drier flue gas (flue gas moisture from 10% to 5%) would results in approximately a 30% increase of mercury oxidation at the APH. This shows that moisture in the flue gas significantly inhibits the mercury oxidation rate.

Therefore, the large flue gas cooling rate and low moisture content of flue gas can contribute to Hg^0 oxidation in the CHX.

Chapter 7

Conclusions

The modeling of elemental mercury oxidation in the condensing heat exchanger (CHX) with Chemkin software was conducted to investigate mercury oxidation in the CHX. Based on the Hg^0 oxidation results of the performance tests of the CHX at Great River Energy, the author modeled the chemical reaction processes to obtain the Hg^0 oxidation results by chemical kinetic calculation tools.

With the limited data collected in the tests done at Great River Energy, parameters like CHX inlet HCl concentration, Hg concentration and SO_3 concentration, etc. were assumed in this investigation. Furthermore, an analytical model of heat and mass transfer processes in the CHX was used to predict flue gas temperatures in the CHX. These new temperature profiles in the CHX gave a different perspective to study Hg^0 oxidation behavior in the CHX.

Some of the conclusions are listed below.

1) Atomic chlorine that plays a key role in Hg^0 oxidation will be generated at furnace and flows downstream with the flue gas.
2) The oxidation reaction between Hg^0 and atomic Cl primarily occurs at temperature 600K to 300K (620°F to 80°F).
3) With increased HCl concentration at the furnace exit and the same temperature profile in the CHX, more Hg^0 will be oxidized before flue gas enters the CHX. In

addition, more Hg^0 will be oxidized within the CHX.

4) The equilibrium calculation shows the oxidized Hg will mainly exist as $HgCl_2$.

5) The simulation shows the Hg^0 oxidation rate will be higher in flue gas containing lower concentrations of water vapor.

6) The lower flue gas temperature and moisture content of flue gas in the CHX will increase the Hg^0 oxidation rate in the CHX.

7) Exact coal ultimate analysis is needed. In the modeling of the report, Hg, HCl and SO_3 concentrations were assumed according to typical values of coal-fired flue gas.

The field tests at Great River Energy and modeling carried by the author both suggest that the CHX would be helpful in reducing mercury emissions. Hg^0 will be oxidized efficiently in the CHX with sufficient HCl in the flue gas. The oxidized Hg will be captured in the condensed water formed in the CHX.

APPENDIX

Table A-1. Geometry of CHX (Bare Tube)

Inputs Parameters							
Heat Exchanger		HX1	HX2	HX3	HX4	HX5	HX6
	Units	Duct Geometry					
Width of Flue Gas Duct	in	14	14	14	14	14	14
Height of Flue Gas Duct	in	6	6	6	6	6	6
Longitudinal Direction # of Row	-	4	6	10	14	14	14
Transverse Direction # of Row	-	8	8	8	8	8	8
Length of HX Section	in	5.13	7.19	11.32	15.45	15.45	15.45
	Units	Tube Geometry					
Transverse Tube Spacing Pitch	in	0.722	0.722	0.722	0.722	0.722	0.722
Longitudinal Tube Spacing Pitch	in	2	2	2	2	2	2
Outside Diameter of Tube	in	0.5	0.5	0.5	0.5	0.5	0.5
Inside Diameter of Tube	in	0.43	0.43	0.43	0.43	0.43	0.43
Staggered or Aligned Tube	-	Align	Align	Align	Align	Align	Align
Calculated Parameters							
Heat Exchanger		HX1	HX2	HX3	HX4	HX5	HX6
	Units						
Heat Transfer Surface Area	ft^2	5.05	7.57	12.59	17.61	17.61	17.61
Cumulative HT Surface Area	ft^2	5.05	12.62	25.21	42.82	60.43	78.04

Table A-2. Mercury Oxidation Chemical Kinetics Mechanism

```
ELEMENTS
C CL H N O HG S
END

SPECIES
HGCL2 HGO HG HGCL
CL2 CLO HCL CL CLO2 COCL HOCL NOCL
O OH O2 O3 H H2 H2O H2O2 HO2 HCO CO CO2
HNO HONO N2 N2O NO NO2 NO3
S SO SO2 SO3
END
```

$$k = Ai*T\hat{}bi *EXP(-Ei/RT)$$

REACTIONS	Ai	bi	Ei	
! H2-O2 Chain Reactions				
2H+M<=>H2+M	1.80E+18	-1.000	0.00	!Edwards
O2/ 0.4/ CO2/1.5/ N2/0.4/ CO/ 0.5/ H2O /6.5/				
2O+M<=>O2+M	2.90E+17	-1.000	0.00	!Edwards
O2/0.4/ CO2/1.5/ N2/0.4/ CO/0.5/ H2O /6.5/				
H+OH+M<=>H2O+M	2.20E+22	-2.000	0.00	!Edwards
O2/0.4/ CO2/1.5/ N2/0.4/ CO/0.5/ H2O /6.5/				
H+O2+M<=>HO2+M	2.30E+18	-0.80	0.00	!Edwards
O2/0.4/ CO2/1.5/ N2/0.4/ CO/0.5/ H2O /6.5/				
2OH+M<=>H2O2+M	3.25E+22	-2.000	0.00	!Edwards
O2/0.4/ CO2/1.5/ N2/0.4/ CO/0.5/ H2O /6.5/				
O2+H<=>OH+O	2.00E+14	0.00	16790.	!Edwards
H2+O<=>OH+H	5.06E+04	2.67	6280.	!Edwards
H2+OH<=>H2O+H	1.00E+08	1.60	3295.	!Edwards
OH+OH<=>H2O+O	1.50E+09	1.14	100.	!Edwards
HO2+H<=>2OH	1.50E+14	0.00	1000.	!Edwards
HO2+H<=>H2+O2	2.50E+13	0.00	690.	!Edwards
HO2+H<=>H2O+O	3.00E+13	0.00	1720.	!Edwards
HO2+O<=>OH+O2	1.80E+13	0.00	-405.	!Edwards
HO2+OH<=>H2O+O2	6.00E+13	0.00	0.0	!Edwards
HO2+HO2<=>H2O2+O2	2.50E+11	0.00	-1240	!Edwards
H2O2+H<=>H2+HO2	1.70E+12	0.00	3750.	!Edwards
H2O2+H<=>H2O+OH	1.00E+13	0.00	3580.	!Edwards
H2O2+O<=>OH+HO2	2.80E+13	0.00	6400.	!Edwards
H2O2+OH<=>H2O+HO2	5.40E+12	0.00	1000.	!Edwards
! CO Reaction				
CO+OH<=>CO2+H	6.00E+06	1.50	-740.	!Edwards
CO+HO2<=>CO2+OH	1.50E+14	0.00	23575.	!Edwards
CO+O2<=>CO2+O	2.50E+12	0.00	47770.	!Edwards
! NOx Reactions				
CO+NO2<=>CO2+NO	1.20E+14	0.00	31600.	!Roesler
NO+O+M<=>NO2+M	4.72E+19	-2.87	1550.	!Mueller
NO+H+M<=>HNO+M	8.95E+19	-1.32	730.	!Roesler
NO+OH<=>HONO	3.65E+14	-2.82	0.00	!Roesler
NO+NO<=>N2+O2	1.30E+14	0.00	75600.	!Roesler
NO+HO2<=>HNO+O2	2.00E+11	0.00	2000.	!Roesler

```
NO2+H2<=>HONO+H                  2.41E+13        0.00        28800.   !Roesler
NO2+O<=>O2+NO                    3.91E+12        0.00         -238.   !Roesler
NO2+H<=>NO+OH                    1.30E+14        0.00          360.   !Roesler
NO2+OH<=>NO+HO2                  1.81E+13        0.00         6670.   !Roesler
NO2+NO<=>N2O+O2                  1.00E+12        0.00        60000.   !Roesler
N2O<=>N2+O                       1.13E+10        0.00        59800.   !Roesler
N2O+O<=>N2+O2                    1.02E+14        0.00        28000.   !Roesler
N2O+O<=>NO+NO                    6.64E+13        0.00        26600.   !Roesler
N2O+H<=>N2+OH                    9.64E+13        0.00        15100.   !Roesler
N2O+OH<=>HO2+N2                  2.00E+12        0.00        10000.   !Roesler
N2O+NO<=>N2+NO2                  1.00E+14        0.00        49600.   !Roesler
HNO+O<=>OH+NO                    3.61E+13        0.00         0.00    !Roesler
HNO+O<=>NO2+H                    5.00E+10        0.00         2000.   !Roesler
HNO+H<=>H2+NO                    1.81E+13        0.00          993.   !Roesler
HNO+OH<=>H2O+NO                  4.82E+13        0.00          993.   !Roesler
HNO+NO<=>N2O+OH                  2.00E+12        0.00        26000.   !Roesler
HNO+NO2<=>HONO+NO                6.02E+11        0.00         1987.   !Roesler
HNO+HNO<=>H2O+N2O                8.43E+08        0.00         3080.   !Roesler
HONO+O<=>OH+NO2                  1.20E+13        0.00         5961.   !Roesler
HONO+OH<=>H2O+NO2                1.26E+10        1.00          135.   !Roesler
!       SOx Reactions
SO3+O=SO2+O2                     4.40E+11        0.00         6100.   !Mueller
SO3+SO=SO2+SO2                   1.00E+12        0.00         4000.   !Mueller
SO2+O+M=SO3+M                    4.00E+28       -4.00         5250.   !Mueller
        H2O/10.0/ N2/1.3/
SO2+OH=SO3+H                     4.90E+02        2.69        23800.   !Mueller
SO2+CO=SO+CO2                    2.70E+12        0.00        43800.   !Mueller
SO+M=S+O+M                       4.00E+14        0.00       107000.   !Mueller
SO+O+M=SO2+M                     2.90E+24       -2.90         0.00    !Mueller
        H2O/10.0/ N2/1.3/
SO+OH=SO2+H                      5.20E+13        0.00         0.00    !Mueller
SO+O2=SO2+O                      6.20E+03        2.42         3050.   !Mueller
SO+SO=SO2+S                      2.00E+12        0.00         4000.   !Mueller
!       SOx-NOx Reactions
SO+NO2=SO2+NO                    8.40E+12        0.00         0.00    !Mueller
SO2+NO2=SO3+NO                   6.30E+12        0.00        27000.   !Mueller
!       HG Reactions
HG+CL2=HGCL2                     3.40E+09        0.00         0.00    !Edwards
HG+O=HGO                         3.40E+09        0.00         0.00    !Edwards
HG+CL=HGCL                       1.95E+13        0.00         0.00    !Edwards
HGCL+CL=HGCL2                    1.95E+13        0.00         0.00    !Edwards
HG+N2O=HGO+N2                    5.08E+10        0.00        59810.   !Cobb
!HG+CL+M=HGCL+M                  9.00E+15        0.50         0.00    !Helble
HG+CL2=HGCL+CL                   1.39E+14        0.00        34000.   !Helble
HG+HCL=HGCL+H                    4.94E+14        0.00        79300.   !Helble
HG+HOCL=HGCL+OH                  4.27E+13        0.00        19000.   !Helble
HGCL+CL2=HGCL2+CL                1.39E+14        0.00         1000.   !Helble
!HGCL+CL+M=HGCL2+M               1.16E+15        0.50         0.00    !Helble
HGCL+HCL=HGCL2+H                 4.64E+03        2.50        19100.   !Helble
HGCL+HOCL=HGCL2+OH               4.27E+13        0.00         1000.   !Helble
!       CL Reactions
2CL+M =CL2+M                     2.20E+14        0.00         1790.   !Edwards
HCL+M=H+CL+M                     4.40E+13        0.00        81685.   !Edwards
HCL+H=H2+CL                      1.80E+12        0.30         3800.   !Edwards
H+CL2=HCL+CL                     6.00E+10        1.00          190.   !Edwards
O+HCL=OH+CL                      6.00E+12        0.00         6545.   !Edwards
O+HOCL=OH+CLO                    6.30E+12        0.00         4370.   !Edwards
O+CL2=CLO+CL                     4.50E+12        0.00         3270.   !Edwards
```

```
O+CLO=CL+O2                             3.30E+08        2.00        190.    !Edwards
OH+HCL=CL+H2O                           2.70E+07        1.65        -215.   !Edwards
OH+CL2=CL+HOCL                          8.40E+11        0.00        1790.   !Edwards
OH+HOCL=H2O+CLO                         1.80E+12        0.00        980.    !Edwards
CL+HO2=HCL+O2                           4.10E+13        0.00        -335.   !Edwards
CL+HO2=OH+CLO                           4.20E+13        0.00        0.0     !Edwards
CL+H2O2=HCL+HO2                         6.60E+12        0.00        1960.   !Edwards
!       NO/CL Reactions
NOCL+M=NO+CL+M                          2.50E+12        0.00        31900.  !Roesler
        NO/1.38/ H2/1.6/ CO2/3.5/
NOCL+CL=NO+CL2                          2.41E+13        0.00        0.00    !Roesler
NOCL+H=NO+HCL                           4.60E+13        0.00        890.    !Roesler
NOCL+O=CLO+NO                           5.00E+12        0.00        3000.   !Roesler
CLO+NO=NO2+CL                           3.85E+12        0.00        140.    !Roesler
HNO+CL=HCL+NO                           8.99E+13        0.00        993.    !Roesler
HONO+CL=HCL+NO2                         5.00E+13        0.00        0.00    !Roesler
END
```

REFERENCE

1. U.S. EPA (United States Environmental Protection Agency). (2010). *EPA's Report on the Environment.* Retrieved from http:// www.epa.gov/ncea/roe/

2. Hall, B., Schager, P., & Lindqvist, O. (1991). Chemical reactions of mercury in combustion flue gases. *Water Air & Soil Pollution*, *56*(1), 3-14.

3. Galbreath, K. C., & Zygarlicke, C. J. (1996). Mercury speciation in coal combustion and gasification flue gases. *Environmental science & technology*,30(8), 2421-2426.

4. Lee, C. W., Kilgroe, J. D., & Ghorishi, S. B. (1998). Mercury control research: Effects of fly ash and flue gas parameters on mercury speciation. NASA, (19980218696).

5. Senior, C. L. et al.. (2000). Gas-phase transformations of mercury in coal-fired power plants. *Fuel Processing Technology*, *63*(2), 197-213.

6. Kramlich, J. C., Sliger, R. N., & Going, D. J. (1997, June). Reduction of inherent mercury emissions in pulverized coal combustion. In DOE Grant DE-FG22-95PC95216, presentation at DOE University Coal Research Contractor's Meeting, Pittsburgh.

7. Senior, C. L., Helble, J. J., & Sarofim, A. F. (2000). Emissions of mercury, trace elements, and fine particles from stationary combustion sources. *Fuel Processing Technology*, *65*, 263-288.

8. Ghorishi, B. Fundamentals of Mercury Speciation and Control in Coal-Fired Boilers; EPA-600/R-98-014 (NTIS PB98-127095); National Risk Management Research Laboratory, U.S. Environmental Protection Agency: Research Triangle Park, NC, 1988.

9. Edwards, J. R., Srivastava, R. K., & Kilgroe, J. D. (2001). A study of gas-phase mercury speciation using detailed chemical kinetics. Journal of the Air & Waste Management Association, 51(6), 869-877.

10. Wang, S. X., Zhang, L., Li, G. H., Wu, Y., Hao, J. M., Pirrone, N., ... & Ancora, M. P. (2010). Mercury emission and speciation of coal-fired power plants in China. *Atmospheric Chemistry and Physics*, 10(3), 1183-1192.

11. Li, Ying. (2004). Impact of boiler operation on mercury emissions in coal-fired boilers. *Theses and Dissertations*. Paper 868. http://preserve.lehigh.edu/etd/868

12. Romero, C. E., Li, Y., Bilirgen, H., Sarunac, N., & Levy, E. K. (2006). Modification of boiler operating conditions for mercury emissions reductions in coal-fired utility boilers. *Fuel*, *85*(2), 204-212.

13. Yan, N. Q., Qu, Z., Chi, Y., Qiao, S. H., Dod, R. L., Chang, S. G., & Miller, C. (2009). Enhanced Elemental Mercury Removal from Coal-Fired Flue Gas by Sulfur− Chlorine Compounds. *Environmental science & technology*, *43*(14), 5410-5415.

14. Procaccini, C., Bozzelli, J. W., Longwell, J. P., Sarofim, A. F., & Smith, K. A. (2003). Formation of Chlorinated Aromatics by Reactions of Cl, Cl2, and HCl with Benzene in the Cool-Down Zone of a Combustor. *Environmental science & technology*, *37*(8), 1684-1689.

15. Procaccini, C., Bozzelli, J. W., Longwell, J. P., Smith, K. A., & Sarofim, A. F. (2000). Presence of chlorine radicals and formation of molecular chlorine in the post-flame region of chlorocarbon combustion. *Environmental science & technology*, *34*(21), 4565-4570.

16. Edgerton, E. S., Hartsell, B. E., & Jansen, J. J. (2006). Mercury speciation in coal-fired power plant plumes observed at three surface sites in the southeastern US. *Environmental science & technology*, *40*(15), 4563-4570.

17. Zhuang, Y., Thompson, J. S., Zygarlicke, C. J., & Pavlish, J. H. (2004). Development of a mercury transformation model in coal combustion flue gas.*Environmental science & technology*, *38*(21), 5803-5808.

18. Hall, B., Schager, P., & Weesmaa, J. (1995). The homogeneous gas phase reaction of mercury with oxygen, and the corresponding heterogeneous reactions in the presence of activated carbon and fly ash. *Chemosphere*, *30*(4), 611-627.

19. Galbreath, K. C., & Zygarlicke, C. J. (1996). Mercury speciation in coal combustion and gasification flue gases. *Environmental science & technology*,*30*(8), 2421-2426.

20. Granite, E. J., Freeman, M. C., Hargis, R. A., O'dowd, W. J., & Pennline, H. W. (2007). The thief process for mercury removal from flue gas. *Journal of environmental management*, *84*(4), 628-634.

VITA

Xingchao Wang was born on November 2, 1987 in Gansu province, China. He studied Thermal Engineering and Power System in Department of Thermal Engineering from 2006 to 2010 at Tsinghua University, China. Xingchao Wang completed his Bachelor of Engineering degree in July 2010 then he worked in Department of Thermal Engineering at Tsinghua University as an assistant engineer. After one year, Xingchao Wang began his graduate studies in Mechanical Engineering and Mechanics at Lehigh University in spring, 2012. He is currently working at the Energy Research Center at Lehigh University and pursuing his PhD degree under the guidance of Dr. Edward K. Levy.